

1 **Soil Moisture–Precipitation Coupling: Observations from the**
2 **Oklahoma Mesonet and Underlying Physical Mechanisms**

3 **Trent W. Ford¹, Anita D. Rapp², Steven M. Quiring¹, Jennifer Blake³**

4 **[1] Department of Geography, Texas A&M University, College Station, Texas**

5 **[2] Department of Atmospheric Sciences, Texas A&M University, College Station, Texas**

6 **[3] Department of Geology and Geophysics, Texas A&M University, College Station, Texas**

7 Correspondence to: T. W. Ford (twford@tamu.edu)

8
9 **Abstract**

10 Interactions between soil moisture and the atmosphere are driven by the partitioning of sensible
11 and latent heating, through which, soil moisture has been connected to atmospheric modification
12 that could potentially lead to initiation of convective precipitation. The majority of previous
13 studies linking the land surface to subsequent precipitation have used atmospheric reanalysis or
14 model datasets. In this study, we link *in situ* observations of soil moisture from more than 100
15 stations in Oklahoma to subsequent unorganized afternoon convective precipitation. We use
16 hourly NEXRAD radar-derived precipitation to identify convective events, and then compare the
17 location of precipitation initiation to underlying soil moisture anomalies in the morning. Overall
18 we find a statistically significant preference for convective precipitation initiation over drier than
19 normal soils, with over 70% of events initiating over soil moisture below the long-term median.
20 The significant preference for precipitation initiation over drier than normal soils is in contrast
21 with previous studies using satellite-based precipitation to identify the region of maximum
22 precipitation accumulation. We evaluated 19 convective events occurring near Lamont,
23 Oklahoma, where soundings of the atmospheric profile at 0600 and 1200 LST are also available.
24 For these events, soil moisture has strong negative correlations with the level of free convection,
25 planetary boundary layer height, and surface temperature changes between 0600 to 1200 LST.
26 We also find strong positive correlations between morning soil moisture and morning-to-
27 afternoon changes in convective available potential energy and convective inhibition. In general,
28 the results of this study demonstrate that both positive and negative soil moisture feedbacks to
29 are important in this region of the United States.

30

31 **1. Introduction**

32 **1.1. Background**

33 Soil moisture is vital to the climate system. Root zone soil moisture in vegetated regions
34 has a significant influence on evapotranspiration rates (Teuling *et al.* 2006; McPherson, 2007) and
35 latent and sensible heat exchange (Dirmeyer *et al.* 2000; Basara and Crawford, 2002; Guillod *et*
36 *al.* 2014). Through the modification of evapotranspiration and moisture transport from the land
37 surface to the atmosphere, soil moisture can impact regional temperature and precipitation.
38 Because of the strong control soil moisture has on sensible and latent heating, studies have focused
39 on the mechanistic modification of atmospheric conditions by the land surface through energy
40 exchange. Findell and Eltahir (2003) derived a convective triggering potential and, combined with
41 a low-level atmospheric humidity index, determined atmospheric potential for convective
42 initiation over relatively wet or relatively dry soils in Illinois. Santanello *et al.* (2009) used
43 observations of soil moisture and atmospheric conditions to describe the modification of
44 atmospheric moisture and energy by the land surface at the hourly time scale. In addition to local-
45 scale interactions, soil moisture-precipitation coupling can be important for meso-scale circulation
46 initiation, particularly over strong meso-scale soil moisture heterogeneity (Taylor *et al.* 2011).
47 Results from these and similar studies suggest that soil moisture anomalies, which drive
48 preferential latent or sensible heating at the surface, can alter low-level atmospheric temperature
49 and humidity such that atmospheric dew point depressions will be generally lower (higher) over
50 wetter (drier) soils.

51 Through its control of surface evaporative fraction (EF), anomalously wet or dry soils can
52 induce modification of the planetary boundary layer (PBL), including changes in the height of the
53 lifting condensation level (LCL) and the level of free convection (LFC) (Brimelow *et al.* 2011).

54 Without consideration of free-tropospheric conditions, afternoon LCL and LFC heights generally
55 decrease with sufficient moisture flux from a wet soil surface, which increases energy available
56 for convection (i.e., CAPE). In turn, relatively dry soils enhance sensible heating at the surface
57 and promote increased LCL and LFC heights (Frye and Mote, 2010a), increasing mixed-layer
58 stability. These mechanisms act as a positive soil moisture feedback, in which convective cloud
59 cover and subsequent precipitation is more probable over a moist land surface than a dry land
60 surface (Findell *et al.* 2011). However, studies have documented an increased probability of
61 convective precipitation over a dry soil surface, partially attributable to dry soils (enhanced
62 sensible heating) resulting in sufficient PBL growth and eroding of strong morning convective
63 inhibition (CIN) (Santanello *et al.* 2009).

64 Ek and Holtslag (2004) demonstrate the interactive roles of soil moisture and free-
65 tropospheric stability on relative humidity tendency and convective cloud development at the PBL-
66 top. Their model simulations show dry (wet) soils combined with weaker (stronger) above-PBL
67 stability enhances the probability of PBL cloud development (Ek and Holtslag, 2004); a finding
68 later corroborated with observations in the Sahel (Westra *et al.* 2012). Gentine *et al.* (2013)
69 integrate the impacts of surface latent and sensible heat flux and free-tropospheric stability into a
70 two-regime framework, specifically a wet-soil advantage regime and dry-soil advantage regime.
71 Under this framework, moist convection occurs earlier over moist surfaces coinciding with strong
72 free-tropospheric stability, and occurs earlier over dry surfaces coinciding with warm, weakly
73 stratified free-tropospheric conditions (Gentine *et al.* 2013). In light of the results of these studies,
74 we could expect unorganized convection to occur over both wet and dry soils, depending on the
75 overlying free-tropospheric conditions.

76 Because soil moisture has a significant impact on atmospheric conditions and the
77 persistence of strong land-atmosphere interactions, it is important for seasonal climate predictions.
78 Meng and Quiring (2010) show that anomalous spring soil moisture in the North American Great
79 Plains influenced the amount of summer precipitation in the Community Atmosphere Model
80 (CAM3). Roundy *et al.* (2013) demonstrated the importance of soil moisture conditions and land-
81 atmosphere coupling in drought monitoring and forecasting in the Southeast U.S. These and other
82 studies suggest that land-atmosphere interactions, modulated by soil moisture, can significantly
83 influence temperature anomalies and potentially, precipitation, and can aid in climate and extreme
84 event forecasting (Douville and Chauvin, 2000; Koster *et al.* 2011).

85 **1.2. Soil Moisture-Precipitation Coupling in the U.S. Southern Great Plains**

86 Although land-atmosphere interactions have considerable impact on regional climate and
87 climate persistence, debate continues as to the sign and strength of these interactions at various
88 scales. Global climate models have identified the U.S. Southern Great Plains as a “hot spot” of
89 land-atmosphere interactions wherein the probability of precipitation responds strongly to land
90 surface conditions (Koster *et al.* 2004). Studies employing soil moisture observations show less
91 consistent results, with some suggesting a wet soil advantage regime in the region (Frye and Mote,
92 2010b; Ford *et al.* 2015), and others providing evidence of a dry soil advantage regime (Santanello
93 *et al.* 2013; Guillod *et al.* 2015). Still other studies show no evidence of soil moisture–precipitation
94 coupling in the Southern Great Plains region, based on *in situ* observation (Phillips and Klein,
95 2014), satellite (Taylor *et al.* 2012), and reanalysis datasets (Findell *et al.* 2011). The lack of a
96 strong, consistent land-atmosphere signal in this region is impeded by the occurrence of both
97 positive and negative soil moisture feedbacks (Findell and Eltahir, 2003b). Additionally, the
98 conflicting results from these and other studies are partially attributable to the breadth of datasets

99 and methodologies employed (e.g., Findell *et al.* 2011; Guillod *et al.* 2014). However, both wet-
100 positive and dry-negative soil moisture feedback on precipitation are potentially relevant in the
101 Southern Great Plains.

102 The lack of consensus from observation-based studies on the sign and strength of soil
103 moisture–precipitation coupling, combined with the strong positive coupling in global climate
104 models precludes solid conclusions as to the relevance of soil moisture–precipitation coupling in
105 the global climate system. Mesoscale studies are uniquely capable of documenting land-
106 atmosphere interactions while simultaneously accounting for region-specific factors that could
107 confound the results. For example, atmospheric stability in the Southern Great Plains region is
108 significantly impacted by the strength and location of the Great Plains Low-Level Jet (Higgins *et*
109 *al.* 1997; Frye and Mote, 2010). This is further complicated by the intrusion of squall lines and
110 frontal systems during the warm season (Raddatz and Hanesiak, 2008), corresponding with
111 conditions unfavorable for surface-induced convection (Matyas and Carelton, 2010). To properly
112 account for these factors, we use a dense network of meteorological monitoring stations with *in*
113 *situ* soil moisture observations, combined with radar-derived precipitation estimates and
114 atmospheric soundings to analyze the soil moisture-precipitation coupling strength in the Southern
115 Great Plains of the United States. Specifically we address whether unorganized convective events
116 *initiate* preferentially over drier or wetter than normal soils in Oklahoma and document how
117 atmospheric conditions prior to convection respond to soil moisture variability.

118 **2. Data and Methods**

119 **2.1. Soil Moisture Data**

120 *In situ* observations of soil moisture are taken from the Oklahoma Mesonet
121 (<http://mesonet.org/>), comprised of over 100 continuously monitoring stations across the state
122 (Illston *et al.* 2008). Campbell Scientific 229-L heat dissipation sensors are deployed at four depths
123 (5, 25, 60, 75 cm) in the soil column and measure matric potential, from which volumetric water
124 content is derived. Mesonet soil moisture observation error is low (Scott *et al.* 2013), and station
125 density in Oklahoma is among the highest in North America.

126 Daily (9:00 a.m. LST) measurements are used to characterize soil moisture conditions on
127 the morning of each convective event. Because volumetric water content is a strong function of
128 site-specific characteristics, we convert daily volumetric water content measurements to
129 percentiles. For this conversion, an empirical cumulative distribution function, comprised of all
130 daily soil moisture observations for a given calendar month, is constructed. Daily observations are
131 then fit to the distribution, and percentiles of the overall distribution are calculated. This means
132 that a daily percentile value on (e.g.) July 5th of 100 represents the wettest soil moisture condition
133 experienced during any July day over the entire study period. The percentiles are then gridded at
134 a 0.25° spatial resolution across the study region. The location of convective precipitation initiation
135 is matched to the soil moisture grid and a corresponding soil moisture value. It is worth mentioning
136 that soil moisture percentiles in this study represent only local temporal variability, and therefore
137 cannot be used to examine the impact of soil moisture spatial heterogeneity on convective
138 precipitation initiation. Soil moisture observations from the 5 cm depth are used in all analyses.

139 **2.2. Precipitation Event Identification**

140 The majority of precipitation in the central United States is caused by frontal activity and
141 mesoscale convective systems (Raddatz and Hanesiak, 2008; Carleton *et al.* 2008). In these cases,

142 moisture is advected into the region by mid-latitude cyclones or fronts (Matyas and Carleton,
143 2010). Therefore, analyzing the influence of soil moisture on those precipitation events will likely
144 result in a weak or nonexistent relationship. For example, Phillips and Klein (2014) found large-
145 scale atmospheric forcings dominated a relatively weak local feedback signal in the Southern Great
146 Plains. Unorganized convection, as defined by Carleton *et al.* (2008), includes isolated convective
147 events that occur in the absence of strong, synoptic-scale atmospheric forcing. Separating these
148 afternoon precipitation events from organized convective events, like MCSs, and those forced by
149 synoptic-scale atmospheric processes will help to remove confounding factors (i.e., noise) and
150 isolate the influence of the land surface (i.e., signal).

151 Capturing individual convective precipitation events, particularly unorganized convection
152 most pertinent to our study, requires datasets with a high spatial and temporal resolution. Taylor
153 *et al.* (2012) identified convective events using the Climate Prediction Center Morphing Method
154 (CMORPH, Joyce *et al.* 2004), a global precipitation dataset with a 3-hour (temporal) and 0.25°
155 (spatial) resolution. Their precipitation event detection methodology (also implemented by Ford
156 *et al.*, 2015 and Guillod *et al.* 2015) identifies the grid cell that resides within a 1.25° x 1.25° box
157 in which the maximum amount of precipitation occurred. It also identifies the grid cell(s) within
158 the same 1.25° x 1.25° box with the minimum amount of precipitation. Compositing soil moisture
159 associated with these locations of maximum and minimum precipitation provides a means of
160 determining whether there is a preference for convective precipitation to fall over relatively wetter
161 or drier land surfaces. The use of CMORPH precipitation is well-suited for global-scale analyses;
162 however the 3-hour temporal resolution precludes the identification of the point of precipitation
163 *initiation*.

164 Our study identifies unorganized convective precipitation events using ground-based
165 Doppler radar from the National Weather Service (NWS) Next-Generation or NEXRAD radar
166 network. NEXRAD includes over 160 S-band Doppler radars in the United States, including 5 in
167 Oklahoma. The NWS produces their Stage IV hourly precipitation product at 4 km spatial
168 resolution using a mosaic of the ground-based radar data that covers nearly all of the contiguous
169 United States (Lin and Mitchell, 2005). The Stage IV product undergoes bias-correction, quality
170 control, and a series of automated algorithms and manual inspection. NEXRAD precipitation
171 products are ideal for characterizing soil moisture-precipitation interactions occurring at sub-daily
172 time scales (Guillod *et al.* 2014).

173 We examined hourly Stage IV radar images of precipitation accumulation from 3 a.m. to
174 8 p.m. each day between May and September, 2002–2012, and manually identified unorganized
175 convective events. The manual identification procedure was completed according to a pre-
176 determined decision tree (Fig. 1), which approximates the classification system of Schoen and
177 Ashley (2011). Schoen and Ashley’s (2011) system classified storms as cellular unorganized, quasi
178 organized, cellular organized, and linear organized, and was based on previous studies examining
179 radar morphology of convective storms (Parker and Johnson, 2000; Klimowski *et al.* 2003). The
180 decision tree process included 5 assessments or queries: (1) the location of precipitation initiation,
181 (2) minimum event size, (3) precipitation rate, (4) shape and (5) propagation of the event. The
182 classification systems attempts to exclude organized convective events. Specifically, organized
183 convective events in our classification were identified as either (1) conglomerates of convective
184 storms arranged in a linear or quasi-linear fashion or line-echo wave pattern, including bow echoes
185 and squall lines, or (2) as individual cells which initiate and propagate in the same vicinity and
186 direction, arranged in a linear or nonlinear fashion (Gallus *et al.* 2008), and that move/evolve with

187 respect to one another. Organized convection is undesirable because it is typically associated with
188 the synoptic-scale atmospheric processes that we are trying to exclude from this study. The desired
189 unorganized storm type was defined as individual cells which initiated, propagated, and evolved
190 independently of each other and were arranged in a nonlinear fashion (Ashely and Gilson, 2009).
191 These systems are typically shorter lived than organized events, and do not develop into or
192 dissipate from more organized convective modes.

193 Manual event identification procedures have advantages and disadvantages. The primary
194 advantage of a manual classification procedure is the ability of the researcher to discern isolated,
195 unorganized cells from those which develop/evolve together or bifurcate from larger systems. The
196 primary disadvantage of such a manual classification methodology is the lack of repeatability.
197 Even with a well-rooted decision tree to guide the classification process, the results are researcher-
198 specific. To test the reproducibility of this study, classification of all events was completed
199 independently by two researchers. There was 72% agreement between the two researchers with
200 regards to event identification. Agreement varied from year to year and month to month, ranging
201 from 50% for 2009 events to 87% for 2007 events, and 63% for June events to 80% for events in
202 September. Qualitatively, it seemed that the most frequent disagreements between researchers
203 were for (1) multiple, isolated systems that initiated at the same time, and (2) systems which
204 initiated in Oklahoma, but could have been associated with systems initiating outside the study
205 region. Overall, there was a reasonable amount of consistency when using this methodology to
206 detect unorganized convective events.

207 Once an unorganized convective event is identified, the location of afternoon precipitation
208 initiation is established as the grid cell in which precipitation is first captured in the radar dataset.
209 This procedure is different from those used by Taylor *et al.* (2012) and Ford *et al.* (in press), as we

210 identify the point of precipitation initiation instead of the region of maximum accumulation. Once
211 the location of precipitation initiation was established for an event, we determined if more than 3
212 mm of precipitation occurred between 3:00 a.m. and noon (LST) of the preceding morning within
213 20 km of the location of initiation. Convective events were retained only if precipitation did not
214 occur or less than 3 mm had accumulated near the location of initiation. Through our precipitation
215 classification methodology, 477 unorganized events were identified by both researchers during the
216 warm season (May–September) between 2002 and 2012 in Oklahoma (Fig. 2). These events were
217 then used to determine if unorganized convection initiates more frequently over wetter or drier
218 than normal soils.

219 **2.3. Atmospheric Conditions**

220 In addition to documenting the frequency of convection over wet and dry soils, we also use
221 a subset of convective events to characterize atmospheric modification by the land surface in
222 greater detail. Soundings of the atmospheric profile allow for direct connection with the underlying
223 land-surface conditions, but are limited in spatial coverage. Therefore, we use atmospheric
224 soundings at 1200 UTC (0600 LST) and 1800 UTC (1200 LST) from the Department of Energy
225 Atmospheric Radiation Measurement facility at Lamont, Oklahoma for the diurnal evolution of
226 atmospheric moisture and energy. In addition to the atmospheric soundings, we also use estimates
227 of latent and sensible heat flux (W m^{-2}) from the Atmospheric Radiation Measurement facility
228 Energy Balance Bowen Ratio system at Lamont, Oklahoma. The instantaneous latent and sensible
229 heat flux estimates at 1800 UTC (1200 LST) are used to calculate EF, which is the percent of
230 incoming solar radiation used for evaporation.

231 Cluster analysis is used with a Ward's linkage and a 4-class maximum to separate events
232 near Lamont. Hierarchical cluster methods, such as the Ward's method have been used frequently
233 for distinguishing precipitation regimes (Gong and Richman, 1995; Ramos, 2001) and other
234 environmental patterns (Allen and Walsh, 1996). The events are clustered based on their morning
235 (0600 LST) convective triggering potential and low-level humidity (e.g. Findell and Eltahir, 2003).
236 Within each cluster of events, we examine changes in atmospheric humidity and temperature, the
237 level of free convection (LFC), and PBL height.

238 The convective environment and stability of the atmosphere associated with each
239 precipitation event is also characterized using profile-integrated convective available potential
240 energy (CAPE) and convective inhibition (CIN). Taylor and Lebel (1998) suggest that soil
241 moisture anomalies can have a significant influence on CAPE, while Myoung and Nielsen-
242 Gammon (2010) find a strong statistical relationship between soil moisture and CIN values in the
243 Southern Great Plains. We calculate CAPE and CIN using the non-virtual surface parcel in this
244 study. Atmospheric stability measures combined with changes in atmospheric humidity and
245 temperature are linked to underlying soil moisture conditions for the events surrounding Lamont.
246 We examine the physical mechanisms coupling the land surface with the atmosphere, potentially
247 leading to convective precipitation. The organization of the results and discussion are presented as
248 follows: section 3 describes the preference for convection to occur over wet or dry soils,
249 connections between soil moisture and atmospheric conditions are presented in section 4, and
250 section 5 provides a summary and discussion of our results with respect to the broader climate
251 community.

252 3. Results

253 3.1. Dry or Wet Soil Moisture Preference

254 The location of precipitation initiation was identified for each precipitation event and is
255 used to determine the soil moisture conditions in that location (grid cell). The soil moisture
256 percentiles underlying all convective events are presented in Fig. 3. The histogram shows a larger
257 number of convective events occurred over drier than normal soils (< 0.5) than over wetter than
258 normal soils (> 0.5). In fact, the three lowest soil moisture bins (0 – 30th percentile) contain the
259 highest number of convective events.

260 We evaluate the statistical significance of the preference for precipitation initiation over
261 dry soils using a bootstrapping methodology adopted from Ford *et al.* (in press). The procedure
262 compares the frequency of convective events over dry and wet soils to the frequency of dry and
263 wet soils from of a sample of 477 randomly selected days (both event and non-event). For the
264 sample days, soil moisture is taken from a randomly chosen grid cell. Frequency distributions
265 generated from the 10,000 iterations of randomly-sampled days are used to assess the likelihood
266 of achieving the ratio of convective events over dry soils to those over wet soils. Based on this
267 evaluation, the number of convective events observed to occur over drier than normal soils is
268 associated with the 99th percentile of the bootstrapped distribution. This means that the probability
269 of obtaining these results by chance is less than 1%. Therefore, we conclude that there is a
270 statistically significant preference for unorganized precipitation to initiate over drier than normal
271 soils. These results suggest the presence of a dry soil advantage regime (e.g., Gentine *et al.* 2013)
272 in which convective cloud development is favored over a dry soil surface with a deep PBL and a
273 weakly-stratified, warm/dry free-troposphere (Huang and Margulis, 2011).

274 The statistically significant preference for precipitation initiation over dry soils is
275 seemingly in direct contrast with the wet preference found in Ford *et al.* (2015). The primary
276 difference between studies is the use of CMORPH for event identification by Ford *et al.* (2015),
277 and NEXRAD radar in the present study. Two important advantages of NEXRAD which may be
278 partly responsible for the contrasting results are: (1) the ability to identify the location of
279 precipitation *initiation* rather than the location of maximum accumulation, and (2) the ability to
280 discern between unorganized and larger-scale organized systems (Guillod *et al.* 2014). For each
281 of the 477 events, we identified both the location of precipitation *initiation* as well as the location
282 of maximum precipitation accumulation. When we substitute the location of maximum
283 accumulation for the location of initiation when compositing soil moisture underlying events, we
284 find an even stronger preference for convection to initiate over dry soils (not shown). This suggests
285 that the lack of agreement between the findings presented here and those in Ford *et al.* (2015) is
286 most likely due to differences in the datasets and methods used to identify events. When the
287 convective events identified in Ford *et al.* (2015) using methods adopted from Taylor *et al.* (2012)
288 were reanalyzed, it was found that large-scale thunderstorms due to frontal activity, low pressure
289 systems, and even tropical storms were grouped together with mesoscale unorganized convective
290 events (Wang *et al.* in review). The ability to detect soil moisture impacts on convective
291 precipitation initiation is hindered when events due to frontal activity and tropical storms are
292 included because these events do not initiate over the study region. The results presented in this
293 study, however, are based on isolating unorganized convective events and identifying the location
294 of precipitation initiation. This gives us confidence in our assessment of the relationships between
295 soil moisture and unorganized convective events.

296 **3.2. Convective Event Spatial Variability**

297 Land cover and land use boundaries have been shown to dramatically impact atmospheric
298 temperature and humidity in Oklahoma (Avissar and Pielke 1989; McPherson *et al.* 2004).
299 Therefore, we investigated whether the unorganized convective events identified in this study
300 show any spatial patterns that are attributable to variations in land cover (Fig. 2). The G-function
301 was used to provide a quantitative measure of spatial randomness (Diggle, 2003; Perry *et al.* 2006).
302 This method examines the cumulative frequency distribution of nearest neighbor distances for all
303 events. The distribution of nearest neighbor distances calculated from the 477 convective events
304 is then compared against the theoretical distribution of distances generated from a sample of
305 randomly generated points that is the same size as the number of events. More specifically, 477
306 points are randomly placed around Oklahoma, and from these points a theoretical nearest neighbor
307 distribution is generated. This random-point generation procedure is iterated 1,000 times to create
308 a robust theoretical distribution of nearest neighbor distances. The 50th, 97th and 3rd percentiles are
309 identified from this distribution and are used to represent the median and the confidence interval,
310 respectively. The confidence interval is used to determine if the observed location of the
311 convective events are spatially random.

312 Fig. 4 shows the cumulative distribution functions of nearest neighbor distances for the
313 observed convective events (blue line), the bootstrapped median (red line) and 95% confidence
314 envelopes (black lines). The nearest neighbor distance distribution from the convective events falls
315 within the confidence intervals at nearly all distances and, therefore, we conclude that they are
316 spatially random. We repeated this analysis for only wet and only dry events, and both groups
317 were also spatially random.

318 Despite our findings of statistically significant spatial randomness, unorganized convective
319 events seem to cluster in the southeast corner of the state. The cluster is coincident with

320 predominantly mixed forest land cover; however, no association can be made between the location
321 of these events and land cover-induced atmospheric modification. Instead the grouping of these
322 events is attributed to increased atmospheric instability in the form of mid-morning CAPE (J kg^{-1})
323 (Fig. 5). Mid-morning (0900 LST) CAPE composited for the events that occur in the southeast
324 corner of the state (Fig. 5a) is shown separately from 0900 LST CAPE composited for all other
325 events (Fig. 5b). Spatial patterns of the composites are very similar, with the exception of increased
326 CAPE in the southeast corner of the state during the clustered events. Increased potential energy
327 and instability increases the probability of convection, and may explain the apparent grouping of
328 events in the southeast corner of Oklahoma.

329 **3.3. Convective Event Temporal Variability**

330 We examine the monthly and inter-annual variability of wet and dry convective events in
331 Oklahoma. Fig. 6a shows the frequency of dry and wet events during each warm season between
332 2002 and 2012, as well as total (May–September) precipitation (mm) for each year, averaged over
333 all Oklahoma climate divisions. Precipitation totals are taken from the National Climate Data
334 Center Climate Divisional Dataset (<http://www.ncdc.noaa.gov/cag/>). The ratio of dry soil events
335 to wet soil events closely follows the total (May–September) precipitation each year. The two
336 years, 2007 and 2008, with more wet soil events than dry soil events experienced the wettest and
337 second wettest seasons over the study period, at 693 and 539 mm, respectively. The years with the
338 highest dry soil to wet soil event ratios (2002, 2006, 2011, 2012) had the four lowest seasonal
339 precipitation totals. The fact that wet soil events tend to occur in wet years and dry soil events tend
340 to occur in dry years is expected because of the direct impact precipitation has on soil moisture,
341 irrespective of any soil moisture feedback. In addition, because our study focuses on the location
342 of convective precipitation initiation, we cannot account for the potential influence of atmospheric

343 persistence and the impact of large-scale atmospheric conditions (e.g., Taylor *et al.* 2011).
344 Therefore, it is important to note that the patterns shown in Fig. 6 might simply depict the impact
345 of precipitation on soil moisture, rather than a wet or dry soil feedback.

346 Interestingly, the total number of events per year does not seem to be connected to the
347 seasonal precipitation totals. A similar number of events occurred in 2011 (28), a very dry year, as
348 in 2008 (29), which was a wet year. However, the lack of correspondence between total seasonal
349 precipitation and the number of convective events could be due to our preferential selection of
350 unorganized convective events. Fig. 6b shows the monthly variability of all unorganized
351 convective events, both dry and wet. Dry events occur more frequently in May and June than July
352 and August, when the number of wet events increases. To better describe the patterns of temporal
353 variability shown in Fig. 6, we combine monthly and annual frequency into one grid (Fig. 7). The
354 top panel in Fig. 7 shows the frequency of all events, while the middle and bottom panels show
355 frequencies of wet and dry events, respectively. The primary conclusion that can be drawn from
356 Fig. 7a is that the unorganized convective events tend to occur most frequently between June and
357 August, coinciding with the peak convective season in the Southern Great Plains (Fritsch *et al.*
358 1986). While Fig. 7a is divided somewhat horizontally between the middle and beginning/end of
359 the warm season, Figs. 7b and 7c are split vertically. The frequency of wet events (Fig. 7b) is
360 relatively consistent from year to year between 2002 and 2006, with August exhibiting the most
361 frequent wet events. This pattern changes in 2007 and 2008, with a considerable increase in wet
362 event frequency for nearly all months, except September and May. These two very wet years are
363 followed by a pattern that is similar to that observed during 2002 to 2006. The increase in wet
364 events in 2007 and 2008 corresponds with a simultaneous decrease in dry events during the same
365 time period. The warm season in 2007 was the 2nd wettest on record in Oklahoma, with total

366 precipitation more than 237 mm above the 30-year mean. Although the same time period in 2008
367 was less anomalous (25th wettest on record), precipitation was still more than 75 mm above the
368 mean. The abundant precipitation during these two warm seasons led to near-saturated soils for
369 the majority of the time and helps to explain why convection initiated preferentially over wetter
370 than normal soils (i.e., atmospheric persistence, Taylor *et al.* 2011).

371 Over the 11-year study there is, on average, a statistically significant preference for
372 precipitation to initiate over drier than normal soils. However, the total number of events and ratio
373 of dry to wet soil events varies considerably on inter-annual and monthly timescales. Wet soil
374 events occurred most frequently in August during years with less-than-normal to normal
375 precipitation. Not surprisingly, seasons with dry and near-normal rainfall conditions coincided
376 with a higher dry to wet event ratio, while convection over wet soils was most frequent during
377 seasons with above normal precipitation totals.

378 **3.4. Atmospheric Pre-Conditioning to Convection**

379 This study has produced a climatology of unorganized convection in Oklahoma and
380 connected the location of initiation with soil moisture conditions. This analysis is useful for
381 improving our understanding of the relationship between soil moisture and the location and timing
382 of convection. In this section we investigate the physical mechanisms that link the land surface
383 and atmosphere. We composited convective events occurring within 50 km of Lamont, Oklahoma,
384 where atmospheric soundings are taken daily at 0600 and 1200 LST. These events were used to
385 quantify the relationship between the land surface and the atmosphere. The 50 km threshold was
386 selected based on the expected representativeness of the atmospheric profile (Potvin *et al.* 2010)
387 over Lamont as well as the spatial autocorrelation of soil moisture in Oklahoma. Convective events

388 were only retained if: (1) they occurred within 50 km of Lamont, (2) afternoon precipitation was
389 also recorded in Lamont, and (3) soil moisture percentiles in the grid cell where convection
390 occurred had the same anomaly (wet or dry) as Lamont. Based on these criteria, 19 events were
391 selected for analysis.

392 The goal of this analysis is to document the differences in atmospheric conditions between
393 0600 and 1200 LST preceding convection and to account for atmospheric preconditioning to
394 convection occurring over wet soils and that occurring over dry soils. We used convective
395 triggering potential (CTP, J kg^{-1}) and low-level humidity (HI_{low} , $^{\circ}\text{C}$), adopted from Findell and
396 Eltahir (2003a), to identify events with a morning atmosphere preconditioned for convection over
397 wet soils, dry soils, or convection regardless of the land surface. CTP is the integrated area between
398 the environmental temperature profile and a moist adiabat from 900 to 700 mb. The HI_{low} is the
399 summation of the dewpoint depression at 950 and 850 mb. The atmospheric levels used for these
400 calculations are taken directly from Findell and Eltahir (2003a) and are assumed to be relevant for
401 Oklahoma.

402 This comparison is important, as morning atmospheric conditions from which dry soils
403 could potentially force convection should be very different than those favoring wet soil-forced
404 convection. Namely, a dry soil surface modifies atmospheric conditions by forcing PBL growth
405 and free-tropospheric air entrainment, while wet soils effect specific humidity within the PBL
406 (Gentine et al. 2013). Preference for afternoon convective cloud development over wet or dry soils
407 will depend on morning PBL depth and the stability, temperature, and moisture of free-
408 tropospheric air (Findell and Eltahir, 2003a; Huang and Margulis, 2011). Therefore morning (0600
409 LST) atmospheric profiles and CTP- HI_{low} conditions over dry and wet soils are expected to be
410 noticeably different. Fig. 8a shows all 19 events composited around Lamont, plotted in dual CTP-

411 HI_{low} space. The scatter plot shows clear separation of the dry and wet soil events, particularly in
412 the vertical (HI_{low}) and to a lesser extent in the horizontal (CTP). Atmospheric conditions prior to
413 convection over wet soils are characterized by an environmental temperature profile relatively
414 close to the moist adiabatic lapse rate, with an average CTP of 139 J kg^{-1} and high humidity at low
415 levels (mean HI_{low} of 10°C). These conditions are similar to the findings of Findell and Eltahir
416 (2003a) for deep convection initiating over wet soils, and are consistent with a wet soil advantage
417 regime (Gentine *et al.* 2013) in which the wet soils impact PBL specific humidity and therefore
418 PBL depth (i.e., dynamic factor). Atmospheric conditions prior to convection over dry soils have
419 much higher CTP values (mean of 313 J kg^{-1}) and higher HI_{low} (mean of 25°C), representing less
420 stability of the free troposphere (Huang and Margulis, 2011). Delineation of morning atmospheric
421 conditions between wet and dry soil convective events (Fig. 8a) is remarkably consistent with wet
422 and dry soil advantage regimes reported by Gentine *et al.* (2013), representing the importance of
423 both surface soil moisture conditions and pre-convective atmospheric thermal stability in
424 determining a wet or dry soil preference (Huang and Margulis, 2011).

425 In addition to the separation of dry and wet events in CTP- HI_{low} space, there appears to be
426 a distinction within dry and wet events (Fig. 8a). We clustered the 19 events using the 0600 LST
427 CTP and HI_{low} and a hierarchical clustering algorithm with the Ward's linkage and a 4-class
428 maximum. Clustering has been shown to be a useful method for distinguishing disparate conditions
429 leading to the different scatter points (Khong *et al.* 2015), and is therefore deemed appropriate
430 here. The result of the clustering is shown in Fig. 8b, which displays a similar scatter plot as Fig.
431 8a, only with points separated into distinct clusters. The 4 clusters span the entire CTP- HI_{low} range
432 and increase in both CTP and HI_{low} , generally from cluster 1 to cluster 4. Interestingly, despite not
433 including soil moisture as a variable for the clustering analysis, the algorithm divided wet events

434 (clusters 1 and 2) from dry events (clusters 3 and 4). The clusters are used to demonstrate the 0600
435 LST to 1200 LST atmospheric modification in terms of underlying soil moisture and the
436 preconditioning of the morning atmosphere to convection over wet or dry soils.

437 **3.5. Physical Connections between Soil Moisture and Atmospheric Conditions**

438 Atmospheric profiles from soundings at 0600 and 1200 LST are used to characterize
439 conditions and modification from the morning to afternoon before convection occurs. At both 0600
440 and 1200 LST, we calculate the LFC (mb), PBL height (m) and surface temperature ($^{\circ}\text{C}$).
441 Additionally for the 0600 LST sounding, we calculate convective temperature ($^{\circ}\text{C}$), the
442 temperature the near-surface must reach for convection to occur in the absence of synoptic forcing
443 mechanisms, to represent the potential for convection given adequate surface heating. We also
444 calculate CAPE and CIN (J kg^{-1}) to characterize atmospheric stability at both sounding times.
445 Large differences are observed between the clusters for all atmospheric measures. Table 1 shows
446 the average LFC height, CAPE, CIN, convective temperature and PBL height from 0600 and 1200
447 LST as well as the average 0900 LST soil moisture percentile for events in each cluster. CAPE
448 (CIN) values are much higher (lower) at both 0600 and 1200 LST for clusters 1 and 2 events,
449 corresponding with relatively wet soils. Additionally, these clusters have relatively lower LFC and
450 PBL heights and much lower 0600 LST convective temperatures. In direct contrast, dry soil events
451 in clusters 3 and 4 are characterized by relatively low (high) CAPE (CIN) values, deeper PBLs
452 and higher LFC heights. However, more interesting than atmospheric conditions at any one point
453 during the day, are the modifications of atmospheric conditions between 0600 and 1200 LST.

454 Fig. 9 shows scatter plots of the soil moisture percentiles and the 1200 LST – 0600 LST
455 difference in (a) LFC height (mb), (b) PBL height (m) and (c) surface temperature ($^{\circ}\text{C}$), delineated

456 by cluster. Additionally, Fig. 9d shows the same scatter plot, only with 0600 LST convective
457 temperature on the y-axis. The drier soils of clusters 3 and 4 correspond to increased LFC height,
458 stronger PBL growth and increased surface air temperature and morning convective temperature.
459 The change in these atmospheric conditions is an ideal example of the thermodynamic effect for a
460 deep boundary layer over strong surface sensible heating, with decreased LCL and LFC height
461 compared to PBL growth (Santanello *et al.* 2011; Gentine *et al.* 2013). In contrast, events from
462 wet soils events of clusters 1 and 2 show limited PBL growth, decreased LFC heights, lower
463 convective temperature, and smaller changes in surface temperature from 0600 to 1200 LST. This
464 is characteristic of a stable PBL moistened by increased latent heating from a relatively wet surface
465 (i.e., dynamic effect, Gentine *et al.* 2013). Despite the small sample size, all of the relationships
466 depicted in Fig. 9 are statistically significant. The coefficients of determination for soil moisture
467 and changes in LFC height, PBL height, surface temperature and convective temperature are 0.26,
468 0.49, 0.60, and 0.53 respectively. Obviously the relationship between soil moisture and near-
469 surface atmospheric temperature is strongest; however, even with varying atmospheric conditions
470 from 19 events, soil moisture percentiles at 0900 LST still explain more than 25% of the variance
471 in LFC height change from 0600 to 1200 LST.

472 Along with changes in the atmospheric temperature and LFC/PBL heights, we also relate
473 soil moisture percentiles from the 19 events to atmospheric stability. Fig. 10a shows scatter plots
474 of soil moisture percentile and the change (difference) in CAPE (Δ CAPE, J kg^{-1}) between 1200
475 and 0600 LST. Fig. 10b shows the same scatter plot, only showing the 1200 LST – 0600 LST
476 difference in CIN (Δ CIN, J kg^{-1}) delineated by cluster. For clarity, negative Δ CIN values represent
477 a decrease in CIN (decrease in stability) between 0600 and 1200 LST. The general relationship
478 between soil moisture and the changes in both CAPE and CIN are positive, with (wet soil) events

479 in clusters 1 and 2 corresponding with larger (smaller) changes in CAPE (CIN). Mechanistically,
480 drier than normal soils enhance sensible heating at the surface, which results in increased near-
481 surface air temperature and heating of the air parcel near the surface (Fig. 9c). The enhanced
482 warming of the surface allows the surface temperature to approach (or to reach) the convective
483 temperature, essentially decreasing CIN values. Wet soils diminish surface heating, which results
484 in a negligible change in CIN between 0600 and 1200 LST. Concurrently, wetter than normal soils
485 provide enhanced moisture flux to the atmosphere through increased latent heating (Ek and
486 Holtslag, 2004; Gentine *et al.*, 2013). This decreases the level of the LFC (Fig. 9a) and increases
487 CAPE throughout the profile. Through the modification of CAPE and CIN, both wet and dry soils
488 have the potential to initiate convection, and in the case of our 19 events, are physically linked to
489 modifications of the atmosphere. The coupling between soil moisture and CAPE/CIN is also
490 statistically significant, with coefficient of determination values of 0.42 and 0.77, respectively.
491 This means that an overwhelming amount of variance in the evolution of CIN between 0600 and
492 1200 LST (77%) is captured by 0900 LST soil moisture percentiles.

493 Gentine *et al.* (2013) delineate positive and negative regions of relative humidity sensitivity
494 to EF, through which convection is induced. We examine our 17 convective events in (1200 LST)
495 potential temperature slope (γ_θ , K km⁻¹) – EF space to determine if we can similarly separate the
496 events into regions of positive and negative relative humidity sensitivity (Fig. 12). Although not
497 as distinct as the separation demonstrated by Gentine *et al.* (2013), the 17 convective events show
498 a delineation along γ_θ – EF space. Mixed layer relative humidity is most sensitive to changes in
499 surface energy flux when evaporation is constrained under a less stable boundary layer and when
500 evaporation is enhanced under a more stratified boundary layer. The convective events are colored
501 in Fig. 12 based on the 5 cm soil moisture percentile underlying the initiation point. Event

502 separation is further demonstrated as wet and dry soil advantage regimes (e.g., Gentine *et al.* 2013),
503 corresponding with positive and negative regions of relative humidity sensitivity, respectively.
504 Overall, the pattern shown in Fig. 12 supports the dual wet soil-dry soil advantage regimes
505 proposed by Gentine *et al.* (2013), and suggest that convective initiation can occur under both
506 regimes in the Southern Great Plains.

507 Through the manual event identification procedure, we were able to quantify individual
508 event duration (hours), average size (pixels), and total precipitation accumulation (mm) (Table 1).
509 We relate these event characteristics to precedent land surface and atmospheric conditions using
510 correlation analysis. All three event characteristics (duration, size, total precipitation) are
511 significantly, negatively related to the change in PBL height (m) between 0600 and 1200 LST.
512 Larger PBL growth (over predominantly drier soils) corresponds with decreased atmospheric
513 relative humidity, which results in events with shorter duration, smaller size, and less overall
514 precipitation. The coefficient of determination between the change in PBL height and duration,
515 size, and total precipitation are 0.22, 0.31 and 0.40, respectively. Two of the three characteristics,
516 duration and total precipitation, are significantly, positively related to CAPE at 0600 LST. Events
517 exhibiting larger CAPE values correspond to longer event duration and more total precipitation,
518 with coefficient of determination values of 0.41 and 0.85, respectively. The soil moisture percentile
519 does not have a statistically significant relationship with any of the event characteristics.

520 **4. Summary and Conclusions**

521 Soil moisture-precipitation interactions have been a major avenue of hydroclimatic
522 research for decades. Previous studies have found evidence of a wet-positive soil moisture
523 feedback in which increased latent heating from a wet soil surface moistens a stable PBL,

524 decreasing surface temperatures, the lifting condensation level, and the level of free convection,
525 and increasing CAPE (Pielke, 2001; Pal and Eltahir, 2003; Ek and Holtslag, 2004; Ferguson and
526 Wood, 2011; Huang and Margulis, 2011). In contrast, other studies have found that anomalously
527 dry soils can impact convective initiation more strongly than wet soils through increased sensible
528 heat flux, a decrease in CIN and increase in PBL height (Santanello *et al.* 2009; Taylor *et al.* 2012).
529 The preference for convective development over relatively dry soils is particularly evident when
530 PBL growth entrains relatively warm, dry air from a weakly stratified free-troposphere (Westra *et*
531 *al.* 2012; Gentine *et al.* 2013).

532 Our results show a statistically significant preference for unorganized convection to occur
533 over drier than normal soils, although there are a non-negligible number of events that occur over
534 wet soils. Importantly, the ability of our analysis to discern between unorganized convection and
535 organized systems associated with frontal passage and low-pressure systems is dependent on our
536 precipitation event identification. Automated event identification algorithms using other datasets,
537 such as CMORPH, tend to lump together unorganized convective events (e.g., those initiating from
538 local-scale processes), with large-scale frontal systems and tropical storms that do not initiate over
539 the region of interest (Wang *et al.* in review). We compare maximum hourly precipitation
540 accumulation between the 477 events identified here using NEXRAD and the 353 events identified
541 in Ford *et al.* (in press) using CMORPH (Fig. 11). The CMORPH events have a significant larger
542 median maximum hourly accumulation rate, as determined using the Kruskal-Wallis test, than the
543 NEXRAD events. However, the largest differences between the datasets are in the right tail of the
544 distribution, with many CMORPH event accumulation rates exceeding 100 mm/hr. The occurrence
545 of extremely large precipitation rates in the CMORPH dataset suggests that events associated with
546 large-scale systems are being included in the 353 events. Therefore, the lack of agreement between

547 the results of this study and previous studies (Taylor *et al.* 2012; Ford *et al.* in press) can be partly
548 attributed to the different data products and methods used for event identification. With these
549 results in mind, we argue that our manual event identification procedure works best for (1)
550 identifying the point of precipitation *initiation* and (2) separating unorganized from organized
551 convective events. Therefore, we have confidence in our assessment of the relationships between
552 soil moisture and unorganized convective events.

553 After compositing 19 events near Lamont, OK where atmospheric soundings observations
554 were available, we found strong connections between soil moisture and atmospheric modification
555 between 0600 LST and 1200 LST. The strongest modification was to CIN and surface air
556 temperature during this time period, as soil moisture explained 77% and 60% of the variance,
557 respectively. Soil moisture has been previously connected to changes in near-surface air
558 temperature in Oklahoma, albeit at much longer time scales (Ford and Quiring, 2014b). Basara
559 and Crawford (2002) also found that the daily evolution of the PBL, including 2 m air temperature,
560 was connected to soil moisture anomalies on clear sky days. The strong connection between soil
561 moisture and CIN is mechanistically consistent with enhanced (diminished) surface heating over
562 dry (wet) soils. Myoung and Nielsen-Gammon (2010) showed that on monthly time scales, CIN
563 was a better determinant to the occurrence of precipitation during the warm season in Texas.
564 However, their results also showed a strong, negative relationship between soil moisture and CIN
565 such that drier than normal soils resulted in stronger CIN values and therefore stronger atmospheric
566 stability (Myoung and Nielsen-Gammon, 2010). The results from our analysis are not necessarily
567 in disagreement because we evaluated the relationship between soil moisture and the 0600 to 1200
568 LST change in CIN. In fact, as Table 1 shows, 0600 LST and 1200 LST CIN values were strongest
569 over dry soils; however, the enhanced surface heating attributable to moisture-limited land surface

570 conditions in these cases allowed for more rapid surface heating and therefore a larger overall
571 decrease in CIN over dry soils. It should be noted that although stronger CIN over drier than normal
572 soils (e.g. Myoung and Nielsen-Gammon, 2010) can be considered a general deterrent for
573 convection, dry soils can also erode strong CIN much more quickly than wetter soils due to
574 increased sensible heating.

575 The results of this study show strong statistical relationships between soil moisture and
576 several atmospheric conditions and stability indices. These relationships are mechanistically
577 consistent with wet-positive and dry-negative feedbacks to precipitation, suggesting that both
578 positive and negative soil moisture feedbacks are relevant in this region of the United States.

579

580

581 **Acknowledgements**

582 We gratefully acknowledge the National Science Foundation (Award numbers: AGS-1056796,
583 BCS-1433881) for funding this work. We would also like to thank the Oklahoma Mesonet for
584 providing soil moisture observations used in this work. Data files from the Mesonet can be
585 obtained online at: http://www.mesonet.org/index.php/weather/category/past_data_files. Finally
586 we would like to thank Dr. Pierre Gentine and an anonymous reviewer for their helpful
587 comments and suggestions.

588

589

590

591

592

593 **References**

- 594 Allen, T. R., and Walsh, S. J.: Spatial and compositional pattern of alpine treeline, Glacier
595 National Park, Montana. *Photogram. Engin. Rem. Sens.*, 62, 1261-1268, 1996.
- 596 Ashley, W. S., and Gilson, C. W.: A reassessment of U.S. lightning mortality, *Bull. Amer.*
597 *Meteor. Soc.*, 90, 1501-1518, doi: 10.1175/2009BAMS2765.1, 2009.
- 598 Basara, J. B. and Crawford, K. C.: Linear relationships between root-zone soil moisture and
599 atmospheric processes in the PBL. *J. Geophys. Res.*, 107, doi: 10.1029/2001JD000633, 2002.
- 600 Berg, A., Findell, K., Lintner, B. R., Gentine, P., and Kerr, C.: Precipitation sensitivity to surface
601 heat fluxes over North America in reanalysis and model data, *J. Hydrometeorol.*, 14, 722-743,
602 doi:10.1175/JHM-D-12-0111.1, 2013.
- 603 Brimelow, J. C., Hanesiak, J. M., and Burrows, W. R.: Impacts of land-atmosphere feedbacks on
604 deep, moist convection on the Canadian Prairies. *Earth Interact.*, 15, 1-29,
605 doi:10.1175/2011EI407.1, 2011.
- 606 Carleton, A. M., Arnold, D. L., Travis, D. J., Curran, S., and Adegoke, J. O., 2008: Synoptic
607 circulation and land surface influences on convection in the Midwest US “Corn Belt” during the
608 summers of 1999 and 2000. Part I: Composite synoptic environments. *J. Clim.*, 21, 3389-3415,
609 doi: 10.1175/2007JCLI1578.1, 2008.
- 610 Diggle, P. J., Ribeiro, P. J., and Christensen, O.: An introduction to model-based geostatistics. In
611 *Spatial statistics and computational methods. Lecture Notes in Statistics 173* (ed. J. Møller), 43-
612 86. Springer, New York, 2003.
- 613 Dirmeyer, P. A., Zeng, F. J., Ducharme, A., Morrill, J. C., and Koster, R. D.: The sensitivity of
614 surface fluxes to soil water content in three land surface schemes. *J. Hydrometeorol.*, 1, 121-134,
615 doi:10.1175/1525-7541, 2000.
- 616 Dirmeyer, P. A., Schlosser, C. A., and Brubaker, K. A.: Precipitation, recycling, and land
617 memory: An integrated analysis. *J. Hydrometeorol.*, 10, 278-288, doi:10.1175/2008JHM1016.1,
618 2009.
- 619 Douville, H., and Chauvin, F.: Relevance of soil moisture for seasonal climate predictions: a
620 preliminary study. *Clim. Dynam.*, 16, 719-736, doi: 10.1007/s003820000080, 2000.
- 621 Ferguson, C. R., and Wood, E. F.: Observed land-atmosphere coupling from satellite remote
622 sensing and reanalysis. *J. Hydrometeorol.*, 12, 1221-1254, doi: 10.1175/2011JHM1380.1, 2011.
- 623 Findell, K. L. and Eltahir, E. A. B.: Atmospheric controls on soil moisture-boundary layer
624 interactions. Part I: Framework development. *J. Hydrometeorol.*, 4, 552-569, doi:10.1175/1525-
625 7541, 2003.

626 Findell, K. L., Gentine, P., Lintner, B. R., and Kerr, C.: Probability of afternoon precipitation in
627 eastern United States and Mexico enhanced by high evaporation. *Nature*, 4, 434-439,
628 doi:10.1038/ngeo1174.

629 Ford, T. W., Rapp, A. D., and Quiring, S. M.: Does afternoon precipitation occur preferentially
630 over dry or wet soils in Oklahoma?, *J. Hydrometeorol.*, doi: 10.1175/JHM-D-14-0005.1, 2015.

631 Ford, T. W., and Quiring, S. M.: Comparison and application of multiple methods for temporal
632 interpolation of daily soil moisture. *Int. J. Clim.*, 34, 2604-2621, doi: 10.1002/joc.3862, 2014a.

633 Ford, T. W., and Quiring, S. M.: In situ soil moisture coupled with extreme temperatures: A
634 study based on the Oklahoma Mesonet. *Geophys. Res. Lett.*, 41, 4727-4734,
635 doi:10.1002/2014GL060949, 2014b.

636 Fritsch, J. M., Kane, R. J., and Chelius, C. R.: The contribution of mesoscale convective weather
637 systems to the warm-season precipitation in the United States. *J. Appl. Clim. Meteor.*, 25, 1333-
638 1345, doi:10.1175/1520-0450, 1986.

639 Frye, J. D. and Mote, T. L.: Convection initiation along soil moisture boundaries in the southern
640 Great Plains. *Mon. Weather Rev.*, 138, 1140-1151, doi:10.1175/2009MWR2865.1, 2010a.

641 Frye, J. D., and Mote, T. L.: The synergistic relationship between soil moisture and the low-level
642 jet and its role on the prestorm environment in the Southern Great Plains. *J. Appl. Meteor.*
643 *Climat.*, 49, 775-791, doi:10.1175/2009JAMC2146.1, 2010b.

644 Gallus, W. A. Jr., Snook, N. A., and Johnson, E. V.: Spring and summer severe weather reports
645 over the Midwest as a function of convective mode: A preliminary study, *Wea. Forecasting*, 23,
646 101-113, doi: 10.1175/2007WAF2006120.1, 2008.

647 Gentine, P., Holtslag, A.A.M., D'Andrea, F., and Ek, M.: Surface and atmospheric controls on
648 the onset of moist convection over land. *J. Hydrometeorol.*, 14, 1443-1462, doi: 10.1175/JHM-
649 D-12-0137.1, 2013.

650 Gong, X., and Richman, M. B.: On the application of cluster analysis to growing season
651 precipitation data in North America East of the Rockies. *J. Clim.*, 8, 897-931, doi:10.1175/1520-
652 0442, 1995.

653 Guillod, B. P., Orlowsky, B., Miralles, D., Teuling, A. J., Blanken, P. D., Buchmann, N., Ciais,
654 P., Ek, M., Findell, K. L., Gentine, P., Lintner, B. R., Scott, R. L., Van den Hurk, B., and
655 Seneviratne, S. I.: Land-surface controls on afternoon precipitation diagnosed from observational
656 data: uncertainties and confounding factors. *Atmos. Chem. Phys.*, 14, 8343-8367,
657 doi:10.5194/acp-14-8343-2014, 2014.

658 Illston, B. G., Basara, J. B., Fiebrich, C. A., Crawford, K. C., Hunt, E., Fisher, D. K., Elliott, R.,
659 and Humes, K.: Mesoscale monitoring of soil moisture across a statewide network. *J. Atmos.*
660 *Ocean. Technol.*, 25, 167-182, doi: 10.1175/2007JTECHA993.1, 2008.

661 Joyce, R. J., Janowiak, J. E., Arkin, P. A., and Xie, P.: CMORPH: A method that produces
662 global precipitation estimates from passive microwave and infrared data at high spatial and
663 temporal resolution. *J. Hydrometeorol.*, 5, 487-503, doi:10.1175/1525-7541, 2004.

664 Khong, A., Wang, J. K., Quiring, S. M., and Ford, T. W.: Soil moisture variability in Iowa, *Int. J.*
665 *Clim.*, doi:10.1002/joc.4176, 2015.

666 Klimowski, B. A., Bunkers, M. J., Hjelmfelt, M. R., and Covert, J. N.: Severe convective
667 windstorms over the Northern High Plains of the United States, *Wea. Forecasting*, 18, 502-519,
668 doi: 10.1175/1520-0434, 2003.

669 Koster, R. D., Dirmeyer, P. A., Guo, Z., Bonan, G., Chan, E., Cox, P., Gordon, C. T., Kanae, S.,
670 Kowalczyk, E., Lawrence, D., Liu, P., Lu, C., Malyshev, S., McAvaney, B., Mitchell, K., Mocko,
671 D., Oki, T., Oleson, K., Pitman, A., Sud, Y. C., Taylor, C. M., Verseghy, D., Vasic, R., Xue, Y.
672 and Yamada, T.: Regions of strong coupling between soil moisture and precipitation, *Science*,
673 305, 1138-1140, doi:10.1126/science.1100217, 2004.

674 Koster, R. D., Mahanama, S. P. P., Yamada, T. J., Balsamo, G., Berg, A. A., Boissarie, M.,
675 Dirmeyer, P. A., Doblas-Reyes, F. J., Drewitt, G., Gordon, C. T., Guo, Z., Jeong, J. H., Lee, W.
676 S., Li, Z., Luo, L., Malyshev, S., Merrfield, W. J., Senevirantne, S. I., Stanelle, T., van den Hurk,
677 B. J. J. M., Vitart, F., and Wood, E. F.: The second phase of the Global Land-Atmosphere
678 Coupling Experiment: soil moisture contributions to subseasonal forecast skill. *J. Hydrometeorol.*,
679 12, 805-822, doi: 10.1175/2011JHM1365.1, 2011.

680 Lin, Y., and Mitchell, K.E.: The NCEP Stage II/IV hourly precipitation analyses: development
681 and applications. *19th Conf. on Hydrology, American Meteorological Society*, San Diego, CA, 9
682 – 13 January 2005, Paper 1.2.

683 Matyas, C. J. and Carleton, A. M.: Surface radar-derived convective rainfall associations with
684 Midwest US land surface conditions in summer seasons 1999 and 2000. *Theor. Appl. Clim.*, 99,
685 315-330, doi: 10.1007/s00704-009-0144-7, 2010.

686 McPherson, R. A.: A review of vegetation—atmosphere interactions and their influences on
687 mesoscale phenomena. *Prog. Phys. Geogr.*, 31, 261-285, doi:10.1177/0309133307079055, 2007.

688 Meng, L. and Quiring, S. M.: Examining the influence of spring soil moisture anomalies on
689 summer precipitation in the US Great Plains using the Community Atmosphere Model version 3.
690 *J. Geophys. Res.*, 115, doi: 10.1029/2010JD014449, 2010.

691 Myoung, B. and Nielsen-Gammon, J. W.: The convective instability pathway to warm season
692 drought in Texas. Part I: The role of convective inhibition and its modulation by soil moisture. *J.*
693 *Clim.*, 23, 4461-4473, doi:10.1175/2010JCLI2946.1, 2010.

694 Pal, J. S. and Eltahir, E. A. B.: Pathways relating soil moisture conditions to future summer
695 rainfall within a model of the land-atmosphere system. *J. Clim.*, 14, 1227-1242,
696 doi:10.1175/1520-0442, 2001.

697 Parker, M. D., and Johnson, R. H.: Organizational models of midlatitude mesoscale convective
698 systems, *Mon. Wea. Rev.*, 128, 3413-3436, doi: 10.1175/1520-0493, 2001.

699 Perry, G. L. W., Miller, B. P., and Enright, N. J.: A comparison of methods for the statistical
700 analysis of spatial point patterns in plant ecology, *Plant. Ecol.*, 187, 59-82, doi:10.1007/s11258-
701 006-9133-4, 2006.

702 Pielke, R. A.: Influence of the spatial distribution of vegetation and soils on the prediction of
703 cumulus convective rainfall. *Rev. Geophys.*, 39, 151–177, doi:10.1029/1999RG000072, 2001.

704 Potvin, C. K., Elmore, K. L., and Weiss, S. J.: Assessing the impacts of proximity sounding
705 criteria on the climatology of significant tornado environments. *Wea. Forecast.*, 25, 921-930,
706 doi:10.1175/2010WAF2222368.1, 2010.

707 Raddatz, R. L., and Hanesiak, J. M.: Significant summer rainfall in the Canadian Prairie
708 Provinces: modes and mechanisms 2000 – 2004. *Int. J. Clim.*, 28, 1607-1613, doi:
709 10.1002/joc.1670, 2008.

710 Ramos, M. C.: Divisive and hierarchical clustering techniques to analyse variability of rainfall
711 distribution patterns in a Mediterranean region. *Atmos. Res.*, 57, 123-138, doi:10.1016/SO169-
712 8095, 2001.

713 Roundy, J. K., Ferguson, C. R., Wood, E.F.: Temporal variability of land–atmosphere coupling
714 and its implications for drought over the Southeast United States. *J. Hydrometeorol.*, 14, 622-
715 635, doi:10.1175/JHM-D-12-090.1, 2013.

716 Santanello, J. A., Peters-Lidard, C. D., Kumar, S. V., Alonge, C., and Tao, W.: A modeling and
717 observational framework for diagnosing local land-atmosphere coupling on diurnal time scales.
718 *J. Hydrometeorol.*, 10, 577-599, doi:10.1175/2009JHM1066.1, 2009.

719 Santanello, J. A., Peters-Lidard, C. D., and Kumar, S. V.: Diagnosing the sensitivity of local
720 land-atmosphere coupling via the soil moisture-boundary layer interaction. *J. Hydrometeorol.*,
721 12, 766-786, doi: 10.1175/JHM-D-10-05014.1, 2011.

722 Santanello, J. A., and Peters-Lidard, C. D.: Diagnosing the nature of land-atmosphere coupling:
723 A case study of dry/wet extremes in the U.S. Southern Great Plains. *J. Hydrometeorol.*, 14, 3-24,
724 doi:10.1175/JHM-D-12-023.1, 2013.

725 Schoen, J. M., and Ashley, W. S.: A climatology of fatal convective wind events by storm type.
726 *Wea. Forecasting*, 26, 109-121, doi:10.1175/2010WAF2222428.1, 2011.

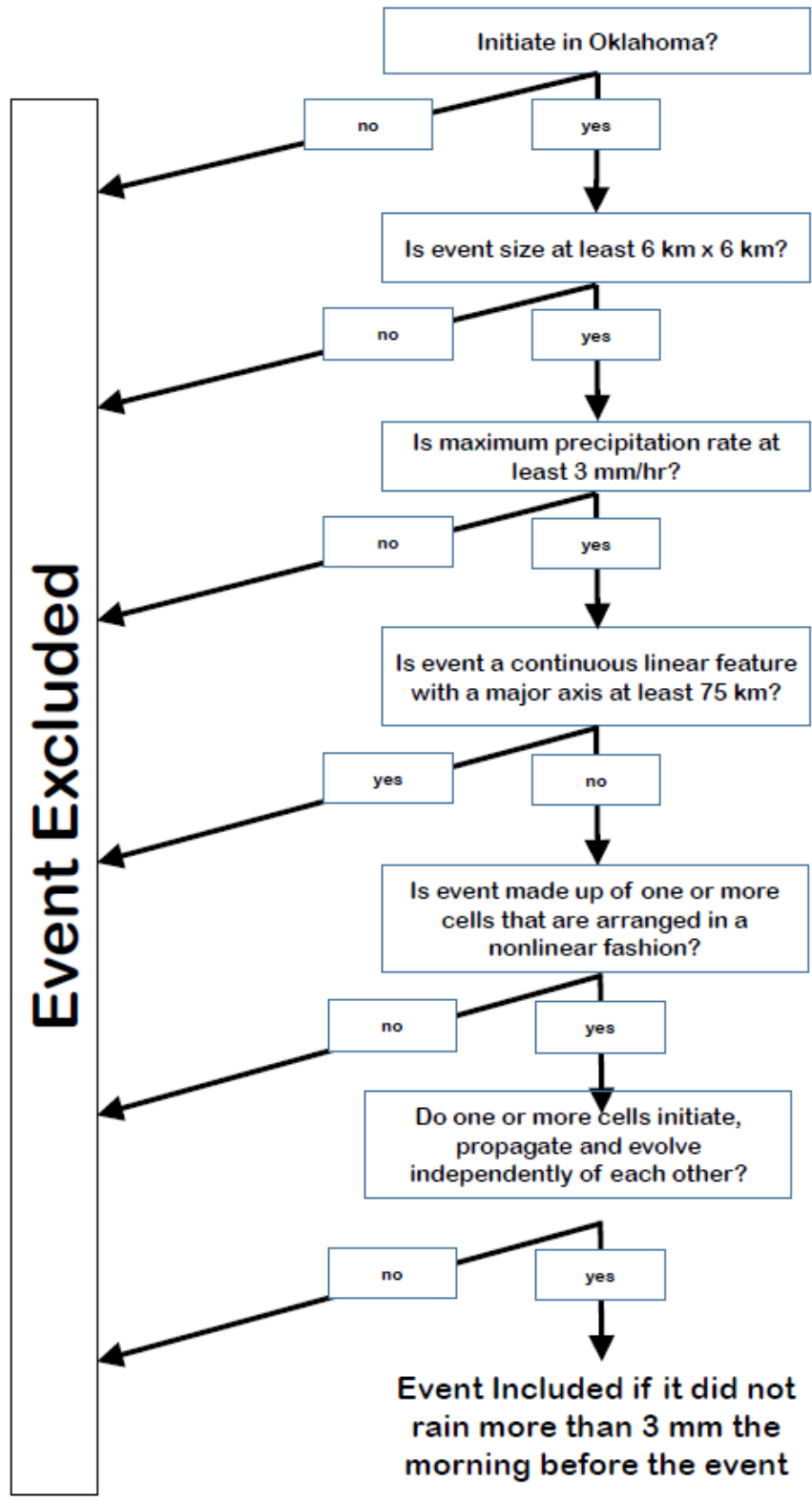
727 Scott, B. L., Ochsner, T. E., Illston, B. G., Fiebrich, C. A., Basara, J. B., and Sutherland, A. J.:
728 New soil property database improves Oklahoma Mesonet soil moisture estimates. *J. Atmo.*
729 *Ocean. Tech.*, 30, 2585-2595, doi: 10.1175/TECH-D-13-00084.1, 2013.

- 730 Seneviratne, S. I., Corti, T., Davin, E. L., Hirschi, M., Jaeger, E. B., Lehner, I., Orlowsky, B.,
731 and Teuling, A. J.: Investigating soil moisture–climate interactions in a changing climate: A
732 review. *Earth-Sci. Rev.*, 99, 125-161, doi:10.1016/j.earscirev.2010.02.004, 2010.
- 733 Taylor, C. M., de Jeu, R. A., Guichard, F., Harris, P. P., and Dorigo, W. A.: Afternoon rain more
734 likely over drier soils, *Nature*, 489, 423-426, doi:10.1038/nature11377, 2012.
- 735 Taylor, C. M. and Lebel, T.: Observational evidence of persistent convective-scale rainfall
736 patterns, *Mon. Weather Rev.*, 126, 1597-1607, doi: 10.1175/1520-0493.
- 737 Teuling, A. J., Seneviratne, S. I., Williams, C., and Troch, P. A.: Observed timescales of
738 evapotranspiration response to soil moisture. *Hydrol. Land Surf. Stud.*, 33,
739 doi:10.1029/2006GL028178, 2006.
- 740 Wu, W. and Dickinson, R. E.: Time scales of layered soil moisture memory in the context of
741 land-atmosphere interaction. *J. Clim.*, 17, 2752-2764, doi:10.1175/1520-0442, 2004.

742

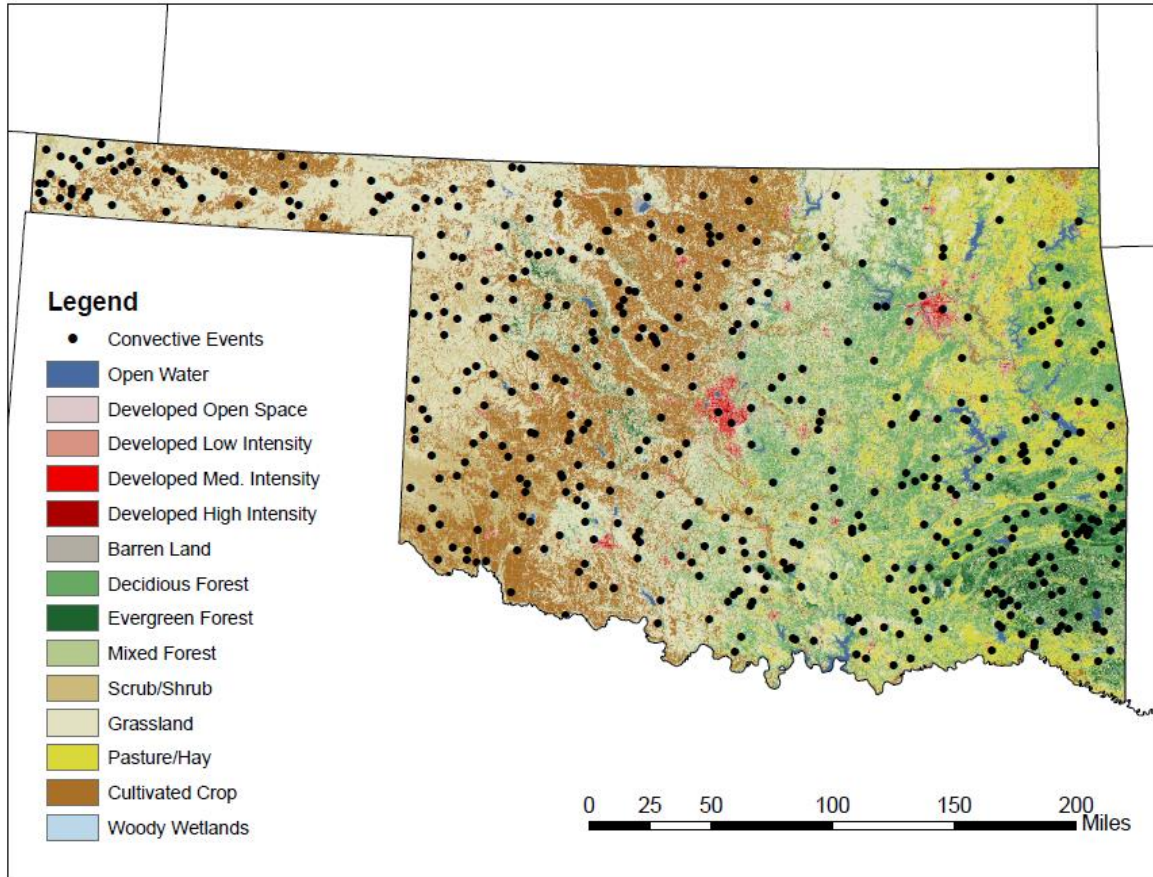
743

744



745

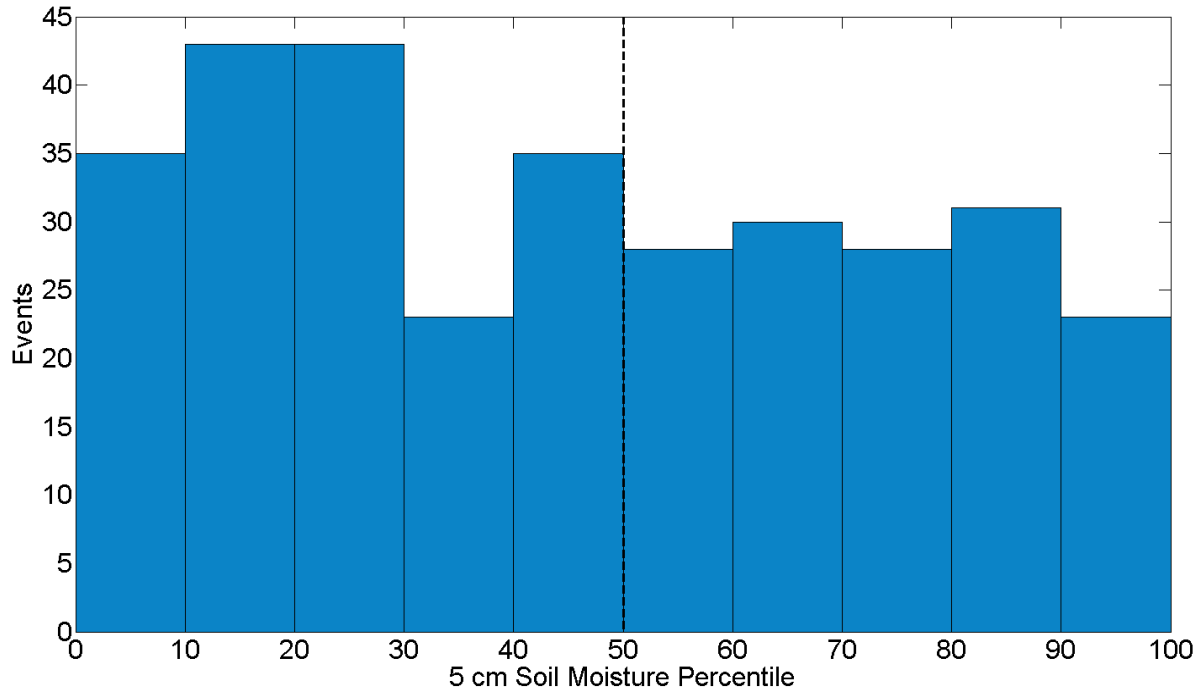
746 **Figure 1.** Schematic of the decision tree that was used for manual identification of unorganized
 747 convective events.



749

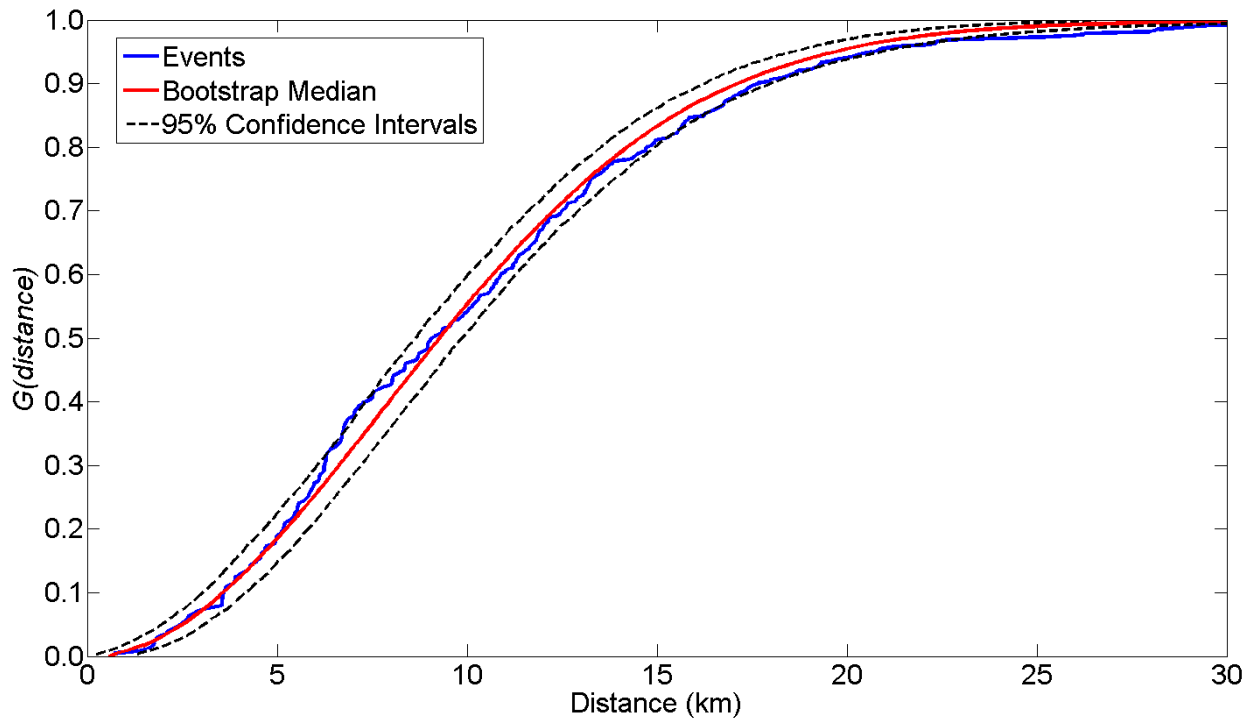
750 **Figure 2.** Location of all 477 convective events (black circles) identified between May and
 751 September, 2002 - 2012. The land cover, taken from the National Land Cover Dataset
 752 (<http://www.mrlc.gov/>), is also shown.

753



754

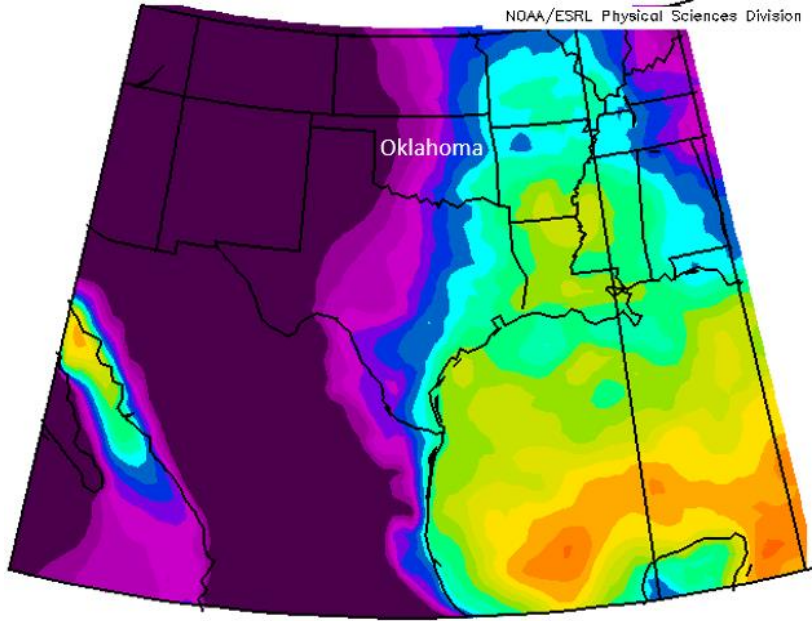
755 **Figure 3.** Top panel (a) shows the distribution of 5 cm soil moisture percentiles underlying all
 756 convective events identified. The dashed-black line represents the divide between relatively wet
 757 (> 50 percentile) and relatively dry (< 50 percentile) soils. The bottom panel (b) shows the
 758 distribution of differences between soil moisture associated with the location of precipitation
 759 initiation and each of the neighboring grid cells in a 3 x 3 window. Negative values represent
 760 conditions where soil moisture was lower at the location of precipitation initiation and higher in
 761 the neighboring grid cell.



762

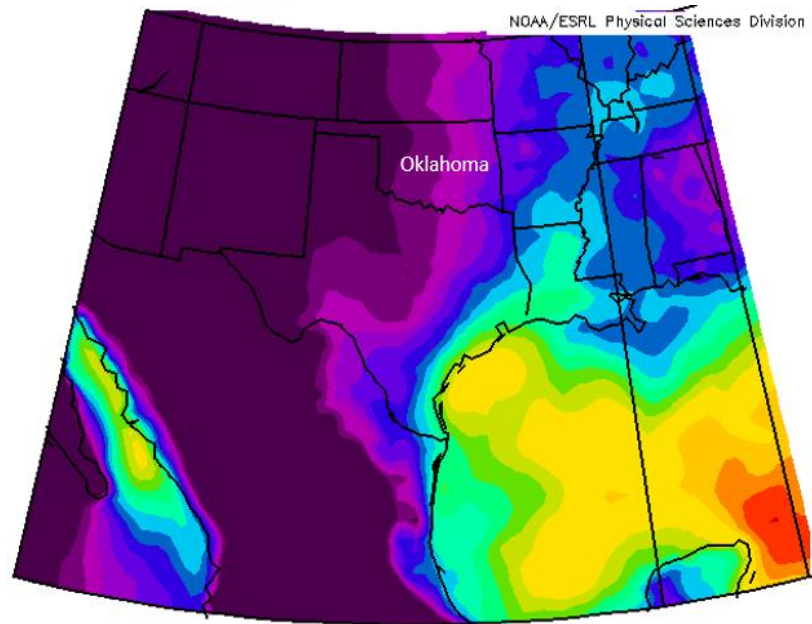
763 **Figure 4.** Cumulative distribution functions of nearest neighbor distances for all unorganized
 764 convective events (blue line), the bootstrapped median (red line) and 95% confidence envelopes
 765 (black lines). The bootstrapped samples are calculated from 1,000 iterations of 477 random
 766 events.

767



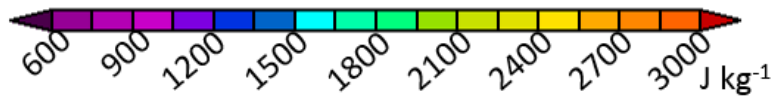
768

a.



769

b.



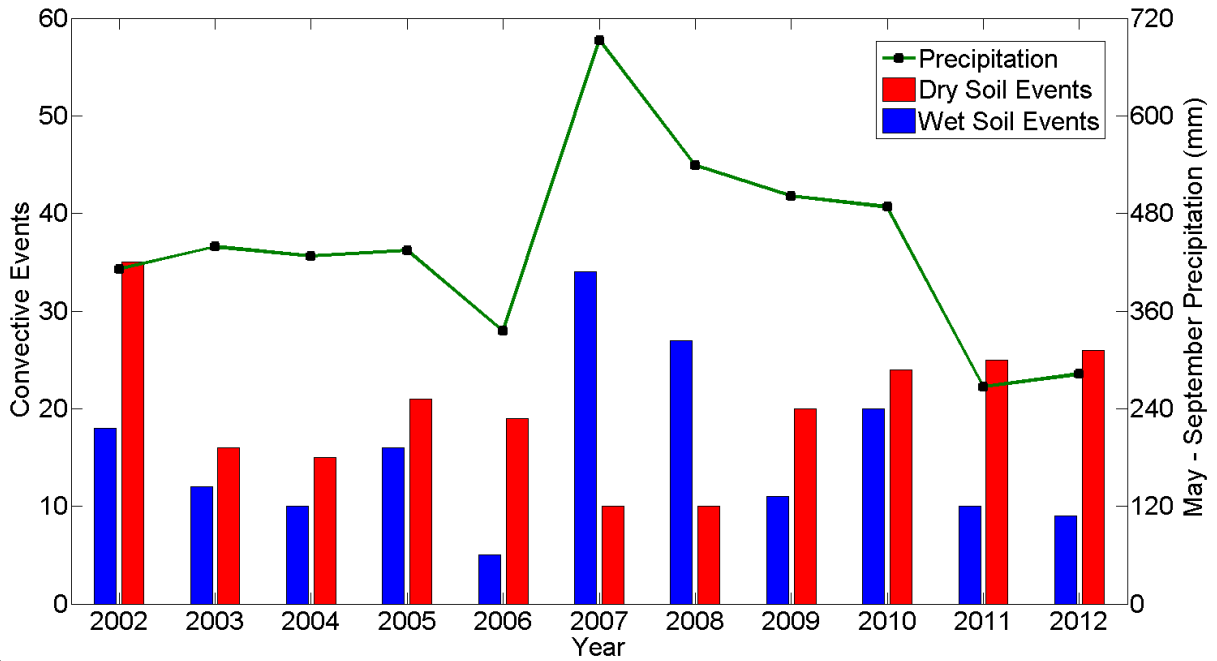
770

771 **Figure 5.** Composites of morning (0600 LST) convective available potential energy from (a)
772 events clustered in southeast corner of the study region and (b) all other convective events.

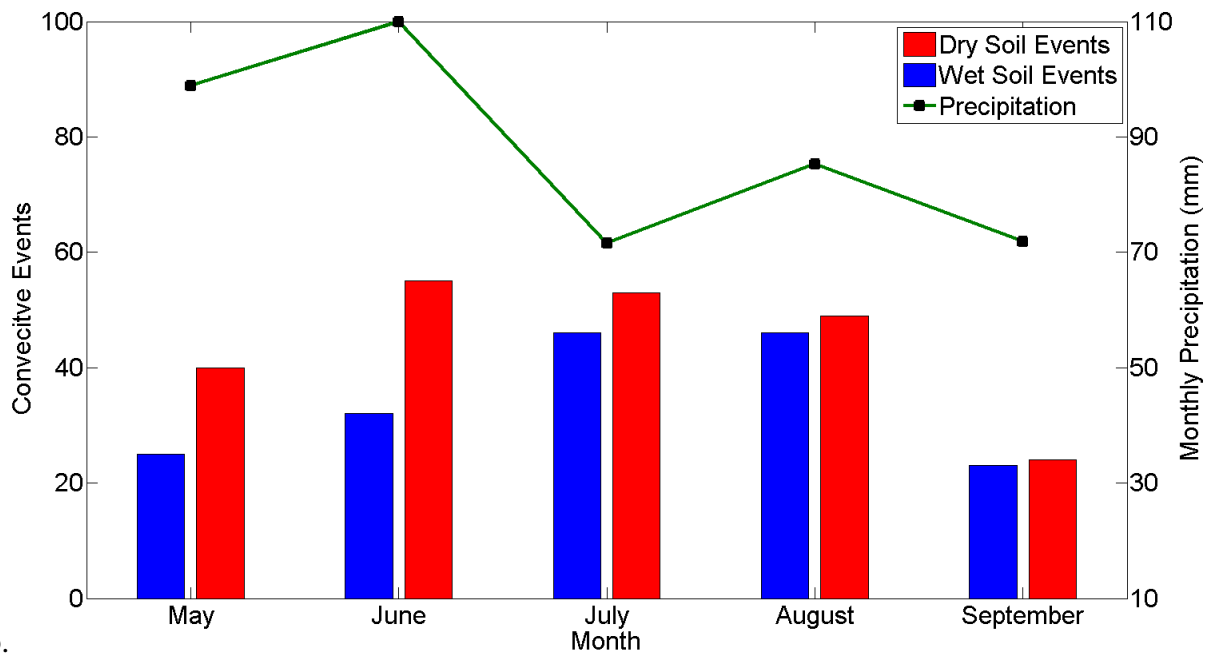
773

774

775



776 a.

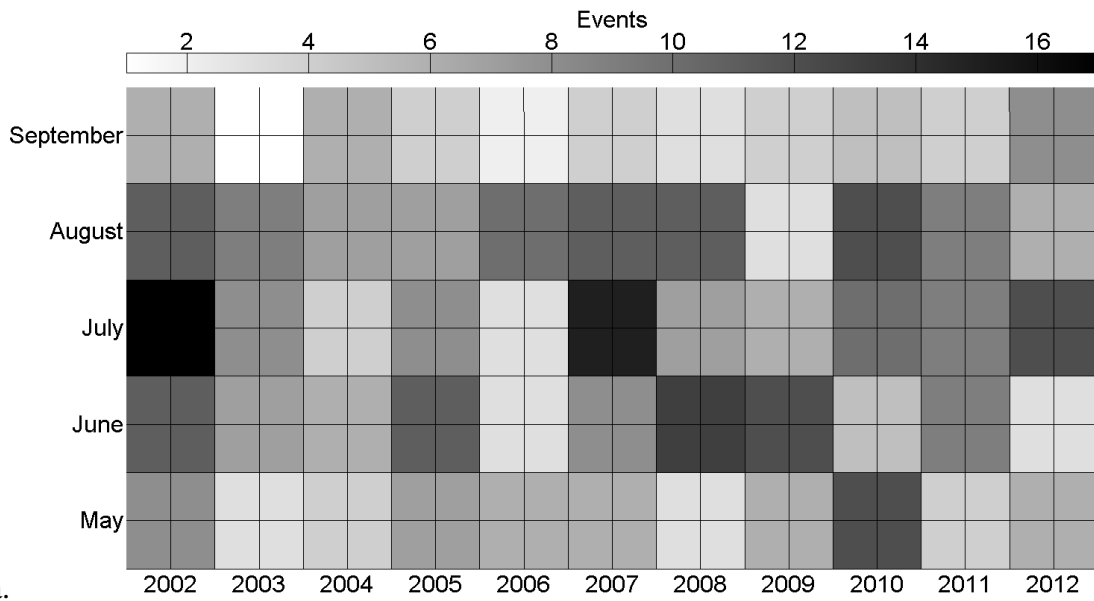


777 b.

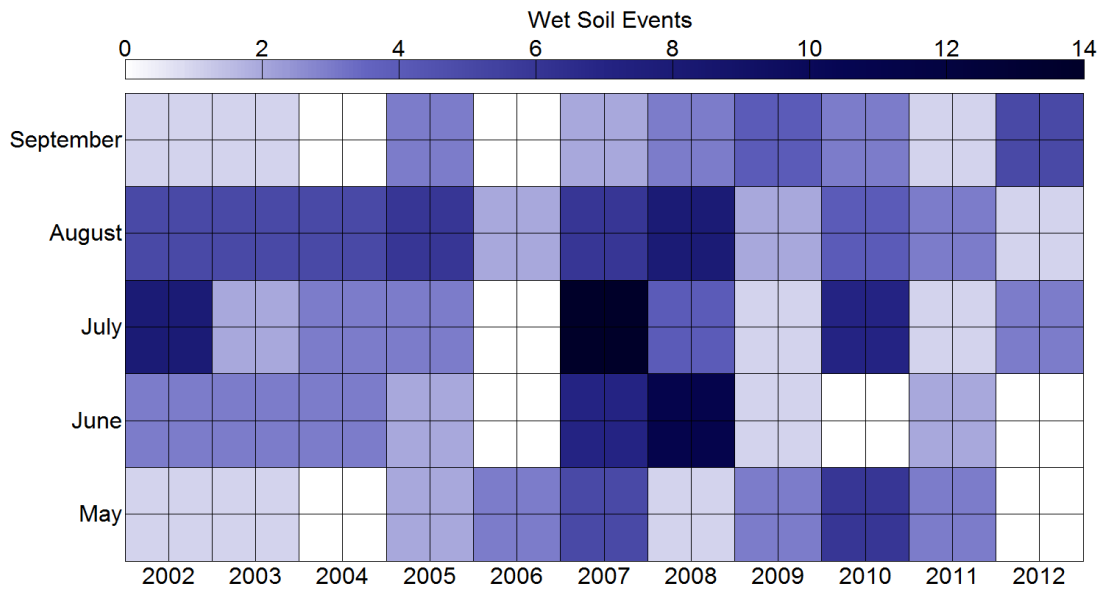
778 **Figure 6.** Top panel (a) shows the frequency of dry and wet events during each warm season
 779 between 2002 and 2012, as well as the total May – September precipitation (mm) for each year.
 780 The bottom panel (b) shows the monthly variability of all events, color-coded into dry and wet
 781 categories, as well as average (2002 – 2012) monthly precipitation (mm).

782

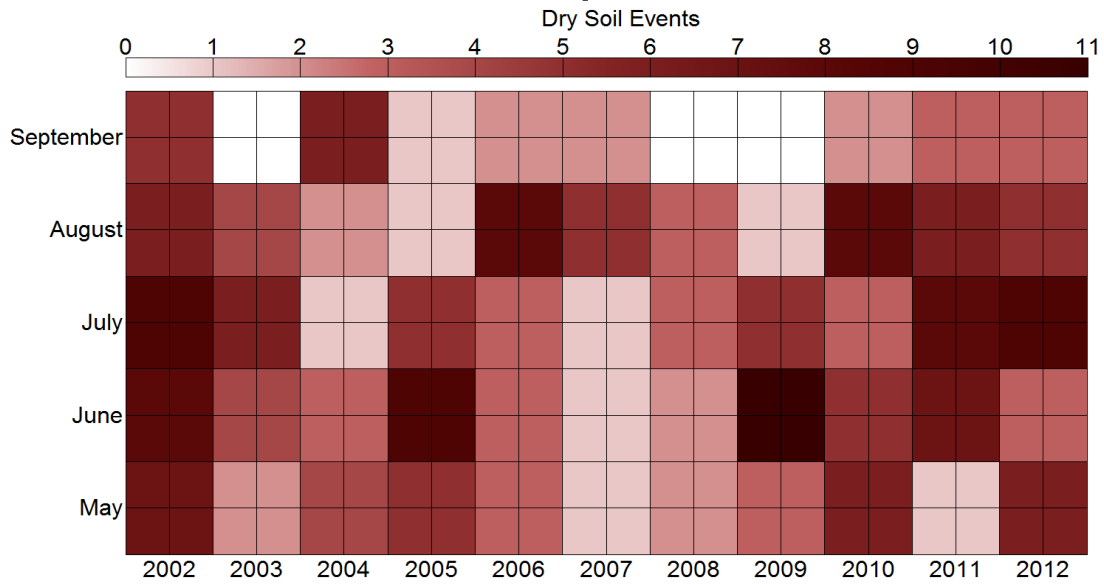
783



784 a.



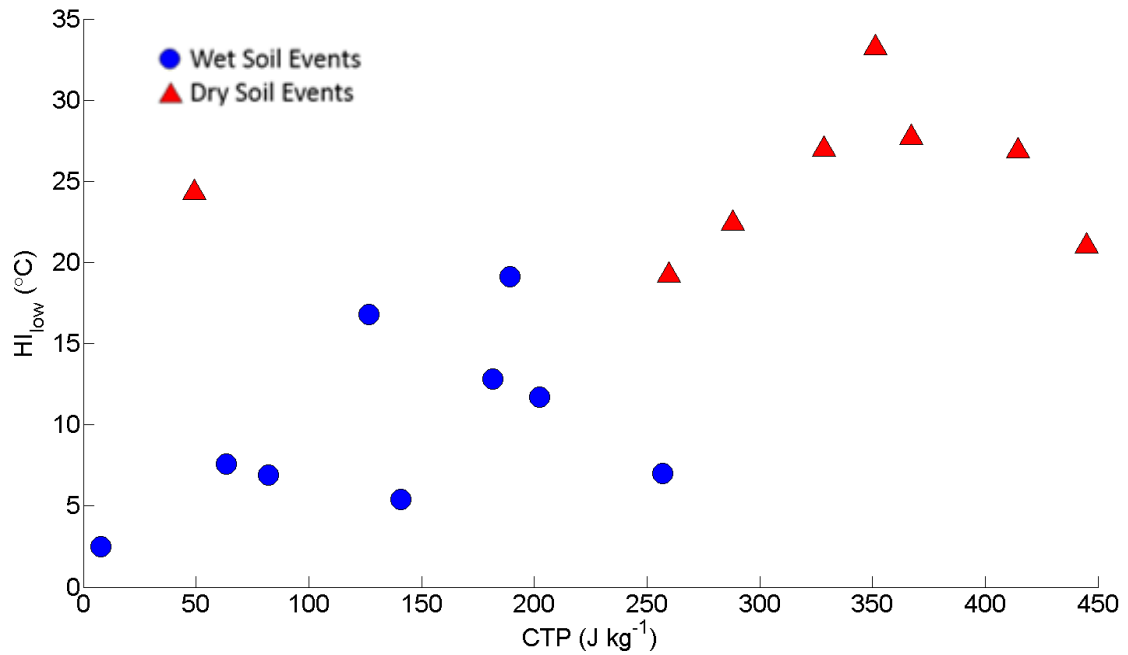
785 b.



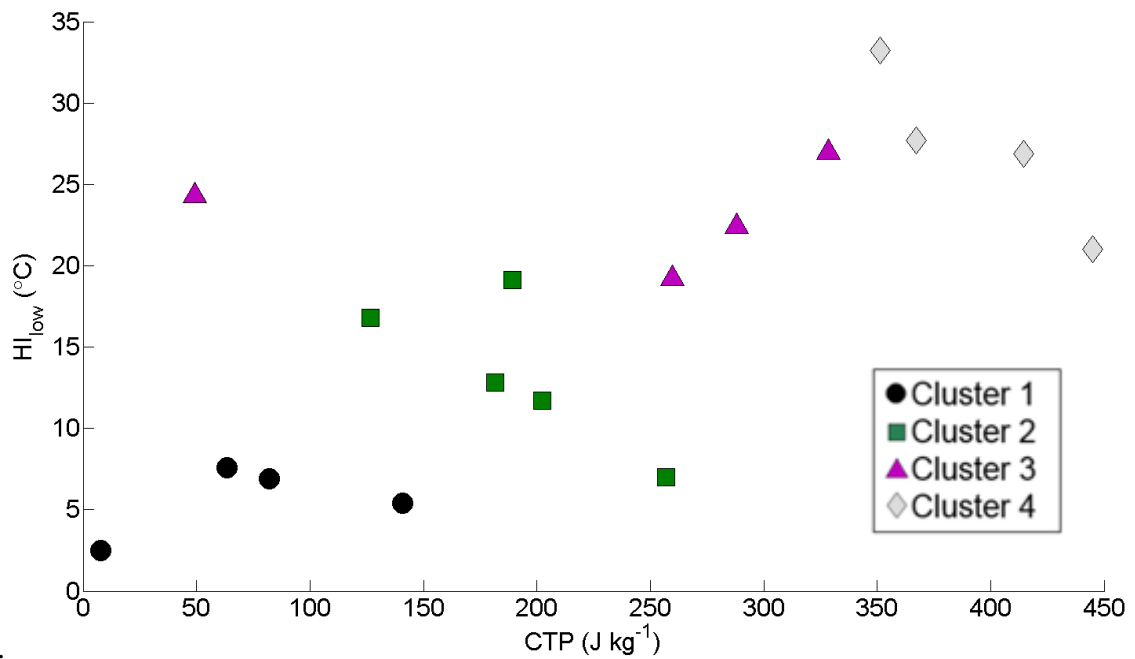
786 c.

787 **Figure 7.** Frequency of unorganized convective events in each month during the 2002-2012
 788 study period. The top panel represents all events, the middle panel is the wet events and the
 789 bottom panel is the dry events.

790

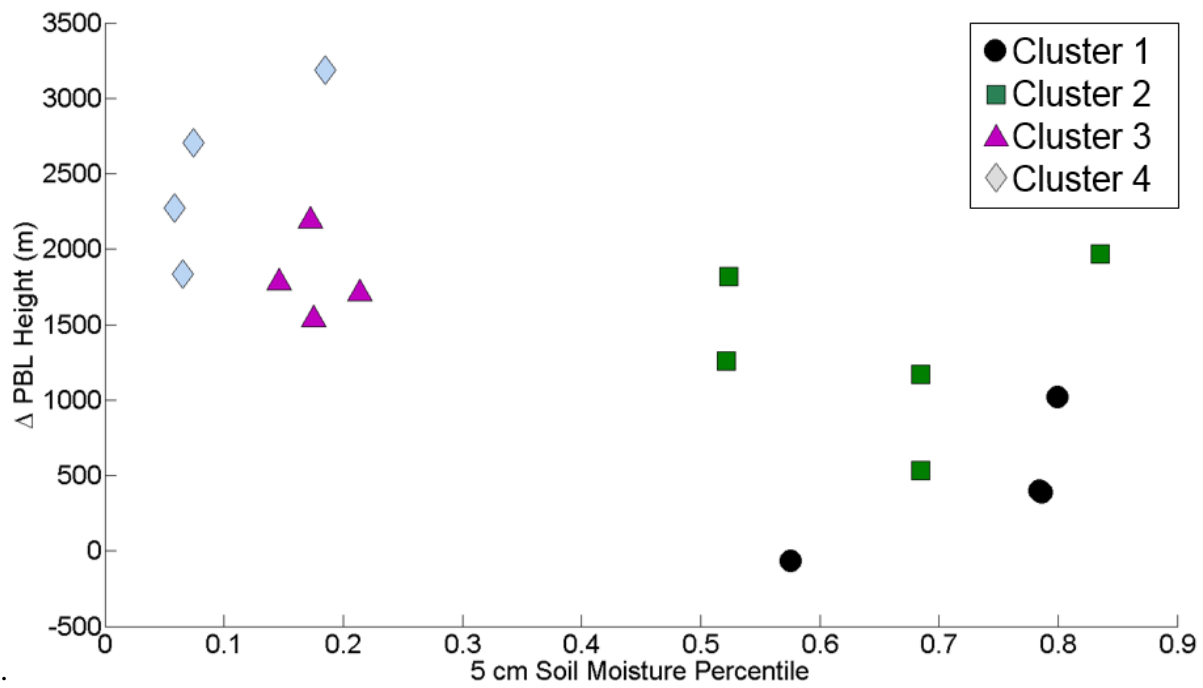
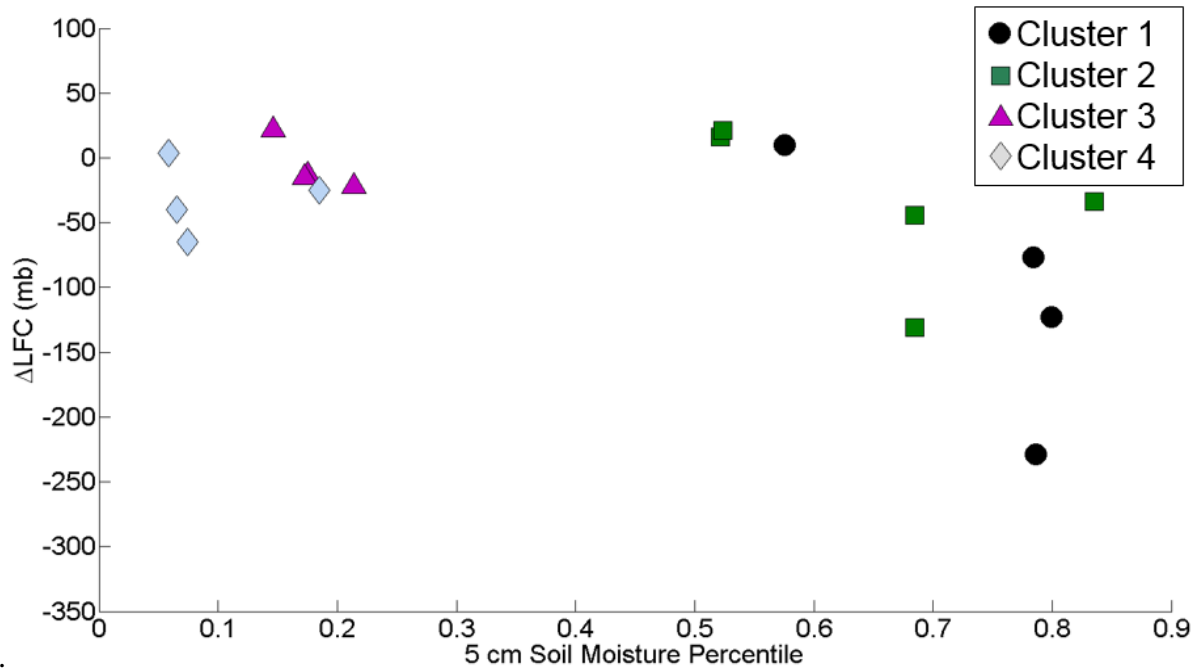


791 a.



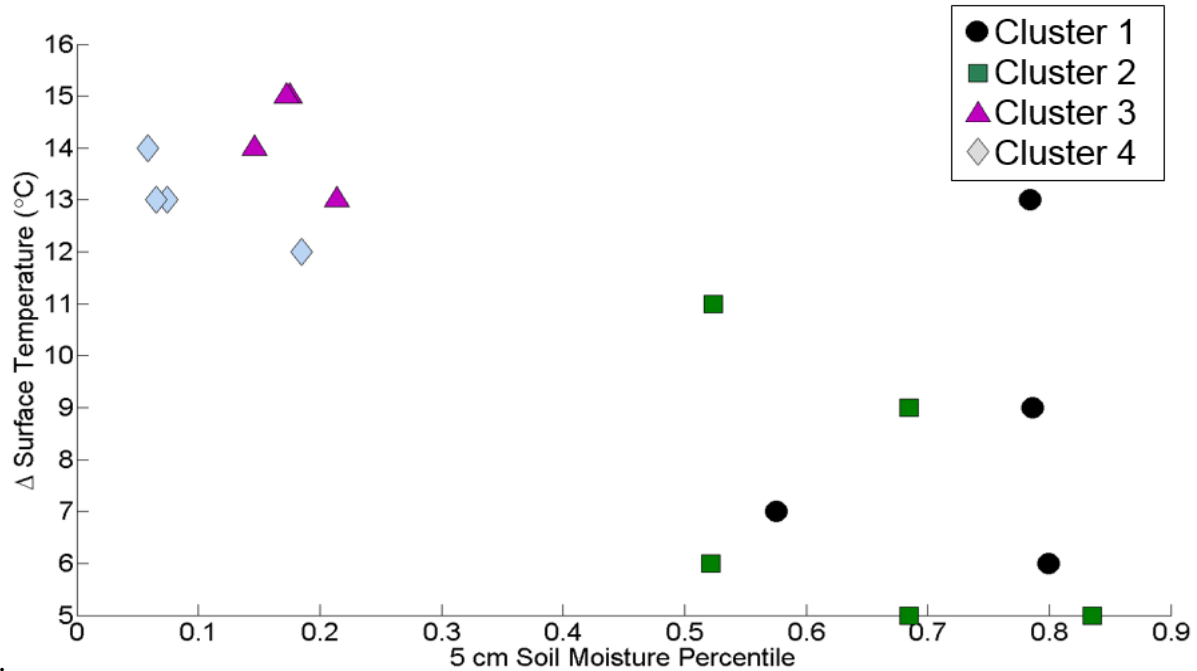
792 b.

793 **Figure 8.** Scatter plots of the 19 unorganized convective events that occurred near Lamont, OK
 794 in dual (0600 LST) convective triggering potential (J kg^{-1}) – humidity index ($^{\circ}\text{C}$) space: (a) wet
 795 events are denoted by the blue circle and dry events are denoted by a red triangle. (b) Events are
 796 grouped into 4 clusters.



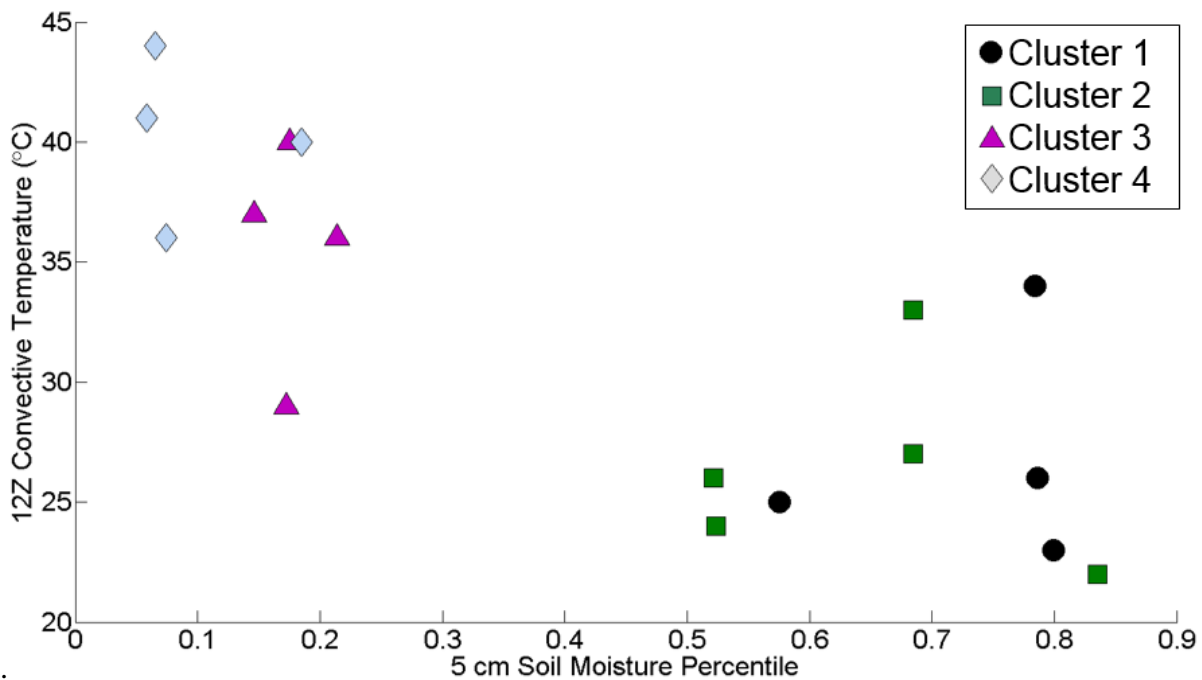
799

c.



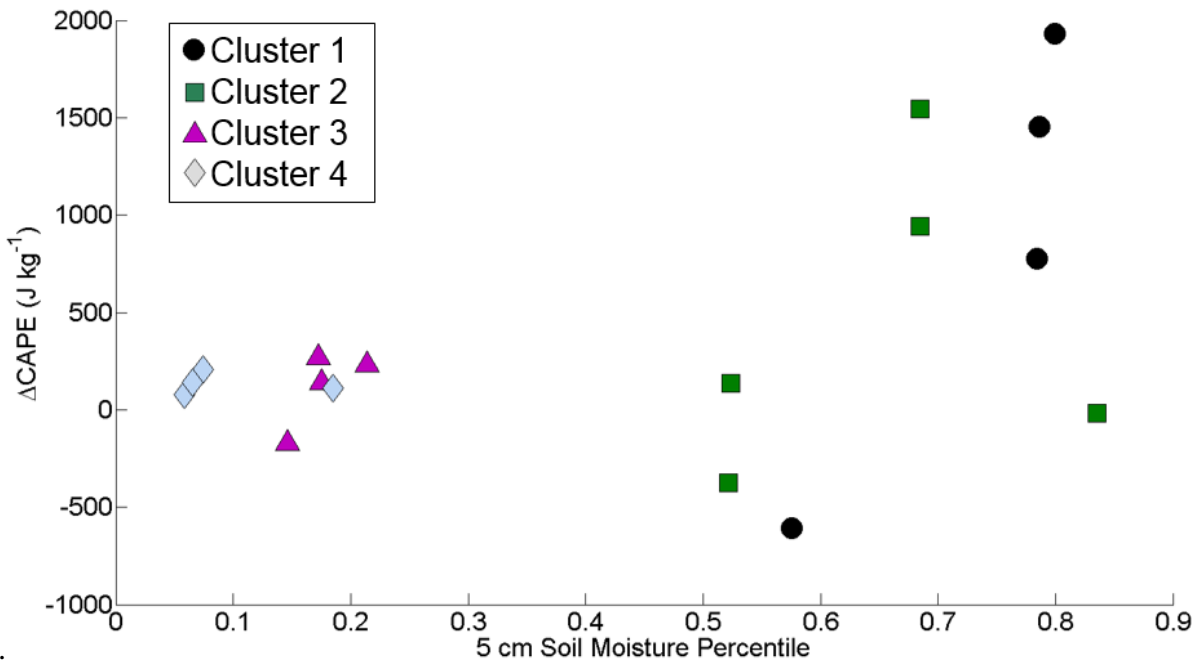
800

d.

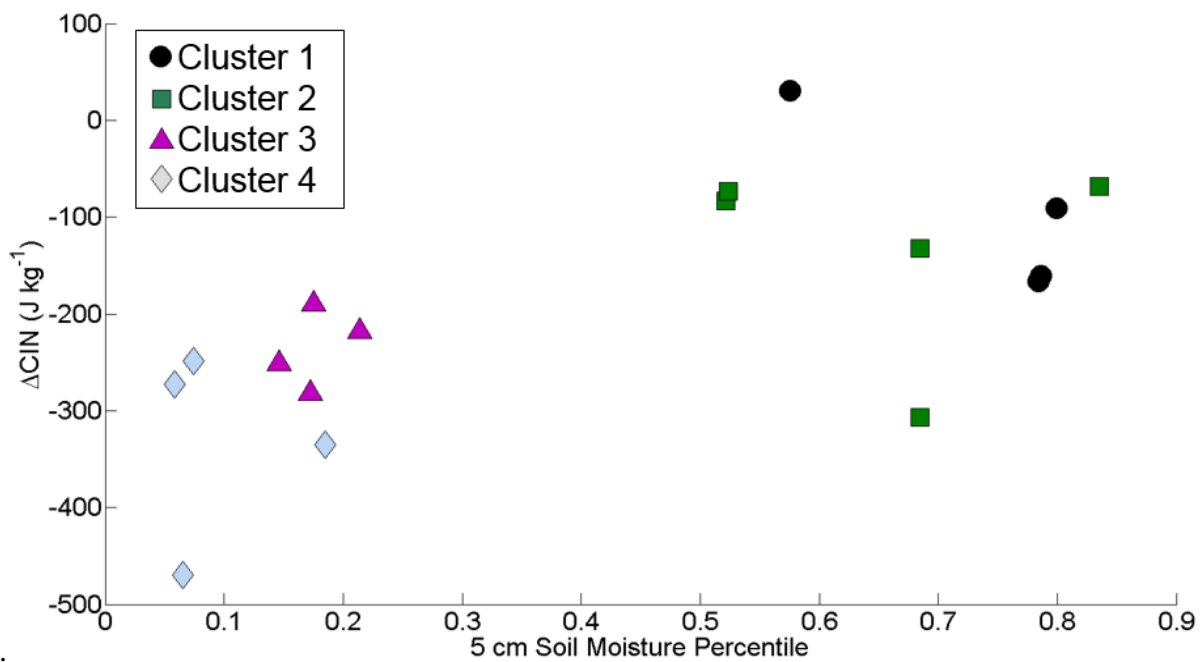


801 **Figure 9.** Scatter plots of soil moisture percentiles and atmospheric conditions 19 unorganized
802 convective events that occurred near Lamont, OK: (a) soil moisture percentiles versus changes in
803 LFC height, (b) soil moisture percentiles versus changes in PBL height, (c) soil moisture
804 percentiles versus surface temperature, and (d) soil moisture percentiles versus 1200 UTC
805 convective temperature.

806



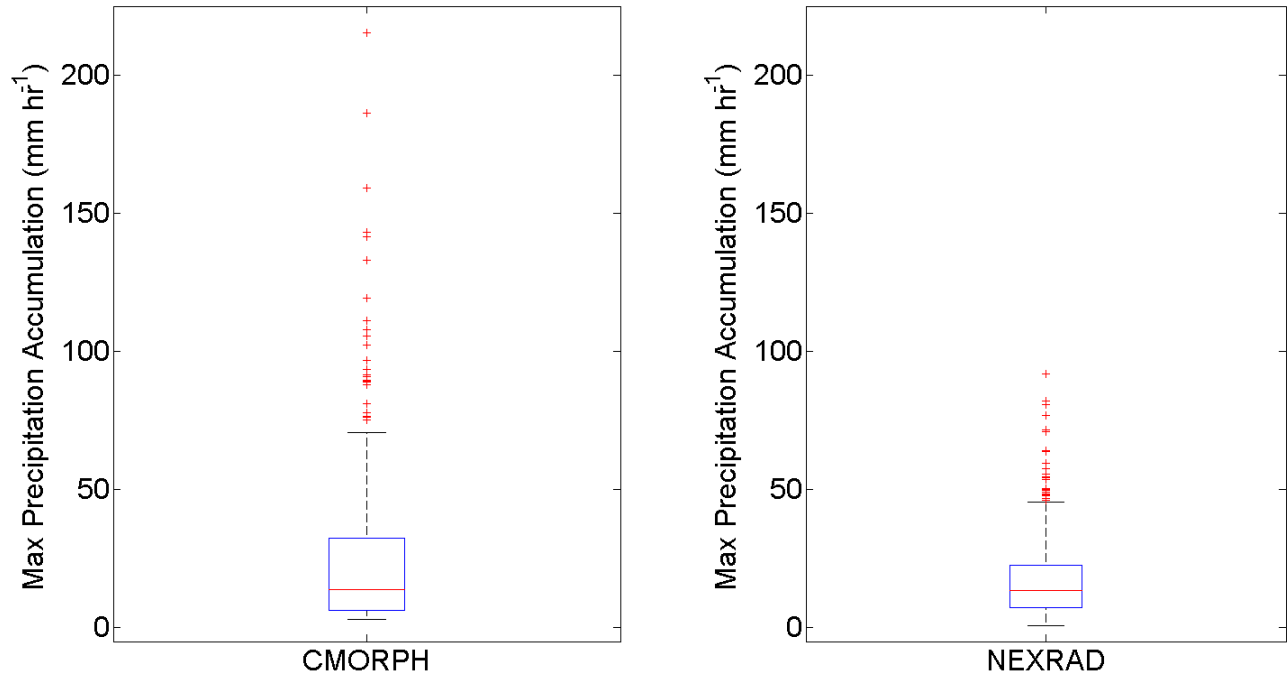
807 a.



808 b.

809 **Figure 10.** Scatter plots of soil moisture percentiles and (a) the change in convective available
 810 potential energy and (b) the change in convective inhibition between 0600 and 1200 LST. Events
 811 shown here occur within 50 km of Lamont, Oklahoma.

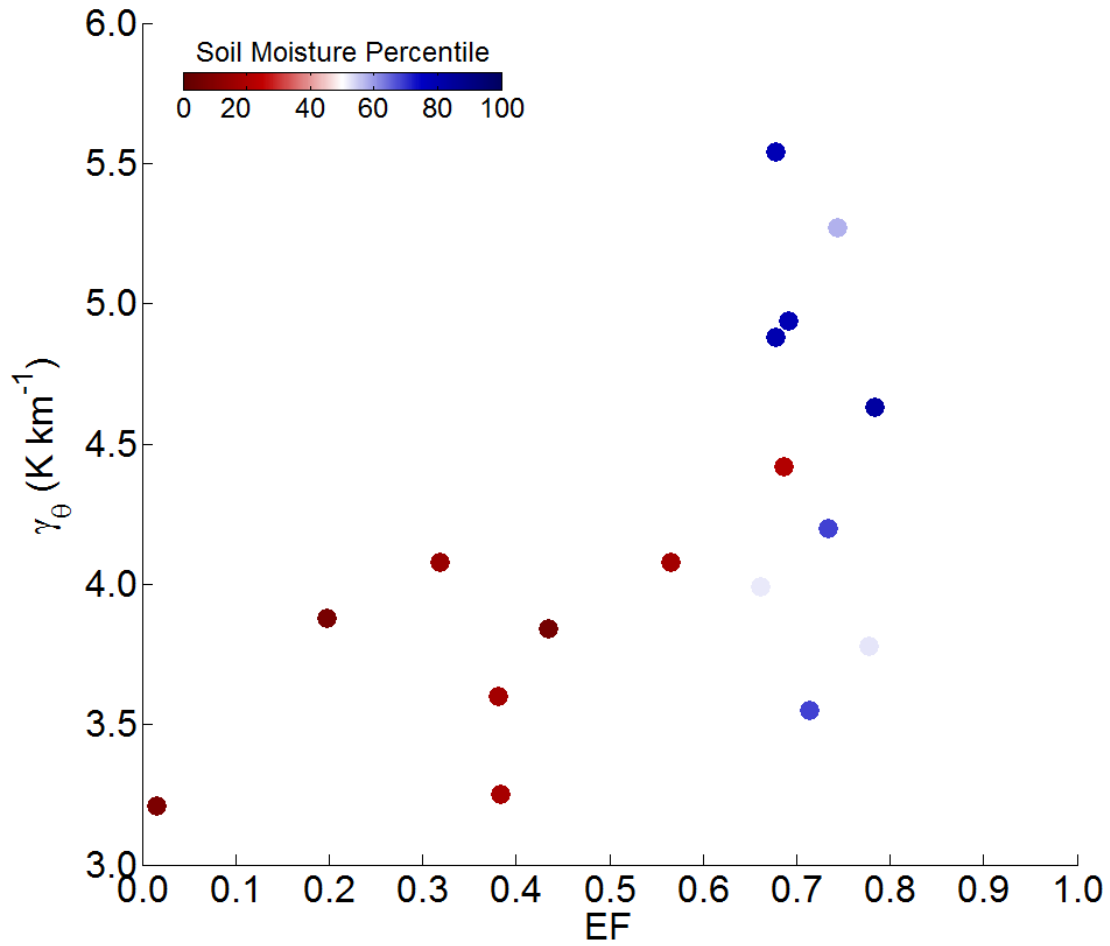
812



813

814 **Figure 11.** Maximum precipitation accumulation rates (mm hr⁻¹) composited from (left panel)
 815 353 events identified by Ford *et al.* (in press) using CMORPH and (right panel) 477 events
 816 identified in this study with NEXRAD.

817



818

819 **Figure 12.** Convective events over Lamont, Oklahoma in terms of 1200 LST atmospheric
 820 stability (γ_θ) and surface evaporative fraction. The scatter points are colored based on the 5 cm
 821 soil moisture percentile underlying each convective event.

822

823 **Table 1.** Mean atmospheric conditions at 0600 and 1200 LST from atmospheric soundings,
 824 averaged by event cluster. Conditions summarized include convective available potential energy
 825 (J kg^{-1}), convective inhibition (J kg^{-1}), the level of free convection (mb), convective temperature
 826 (C), and the height of the planetary boundary layer (m). Mean convective event duration (hrs),
 827 size (pixels) and precipitation accumulation (mm) are composited by cluster as well.

Cluster	1	2	3	4
Soil Moisture (percentile)	0.74	0.65	0.18	0.10
CAPE-12Z (J kg^{-1})	1634.50	686.60	366.75	96.50
CAPE-18Z (J kg^{-1})	2522.50	1133.00	485.00	231.00
CIN-12Z (J kg^{-1})	144.70	190.20	324.00	426.50
CIN-18Z (J kg^{-1})	48.12	57.60	88.75	94.75
LFC-12Z (mb)	717.50	730.20	649.75	594.75
LFC-18Z (mb)	822.25	764.60	656.75	626.25
ConvTemp-12Z ($^{\circ}\text{C}$)	27.00	26.40	35.50	40.25
PBL-12Z (m)	305.26	438.98	370.02	629.00
PBL-18Z (m)	743.70	1788.28	2173.84	3128.63
Event Duration (hrs)	4.25	3.25	3.75	2.75
Event Size (pixels)	23.00	10.75	18.5	7.25
Total Event Accumulation (mm)	1748.05	395.97	546.40	77.66

828

829

830